Heel Buildup during Electrothermal Regeneration of Activated Carbon Fiber Cloth

by

Saeid Niknaddaf

A thesis submitted in partial fulfillment of the requirements for the degree of

Master of Science

In Environmental Engineering

Department of Civil and Environmental Engineering
University of Alberta

ABSTRACT

Adsorption is the most common method for controlling volatile organic compounds (VOCs) emission from automotive painting process. However, unwanted accumulation of adsorbate during cycling (heel buildup) is a common challenge in this process. The objective of this research is to identify the impact of regeneration conditions such as temperature, heating rate and purge flow rate on heel buildup and adsorption capacity. For this purpose, five cycle adsorption/regeneration experiments using 1,2,4-trimethylbenzene (TMB) on activated carbon fiber cloth (ACFC) were completed using resistive heating. Increasing temperature from 288 to 400 °C worsened adsorbent performance, as indicated by smaller adsorption capacity and larger heel buildup. Decreasing heating rate from 100 to 5 °C/min and increasing flow rate from 5 to 0.1 SLPM decreased heel buildup (by 56% and 90%, respectively) and capacity loss (by 85% and 97%, respectively). These observations are the result of carbon deposition due to thermal degradation of TMB during regeneration which is the impact of rapid adsorbent heating rates. The results of this work will help to optimize regeneration condition to allow fast desorption with minimal adsorbate decomposition.

DEDICATION

I would like to dedicate this thesis to my lovely wife, Abedeh, that this success could not be achieved without her endless love, encouragement and support.

ACKNOWLEDGMENTS

First and foremost, I would like to express my sincere gratitude to Dr. Zaher Hashisho for supervision, guidance, and support through my course work and research. His expertise and knowledge were essential for accomplishing this work.

I gratefully acknowledge financial support from Ford Motor Company and the Natural Science and Engineering Research Council (NSERC) of Canada. I also acknowledge infrastructure and instrument grants from Canada Foundation for Innovation (CFI), NSERC, and Alberta Advanced Education and Technology.

I would like to thank my colleagues in air quality and control research characterization laboratory for their assistance, availability and suggestions in my experiments.

I would like to appreciate Dr. John D. Atkinson for his revisions and recommendations to improve this document.

Table of Contents

List of Tables

List of Figures

CHAPTER 1 INTRODUCTION

1-1. Background

Volatile organic compounds (VOCs) include aromatic hydrocarbons, esters, ketones, alcohols, and other organic compounds with a wide range of molecular weights and boiling points (< 260°C) (Golovoy et al. 1981, Kim 2011, Kennes et al. 2013). Depending on how VOCs affect the human health or surrounding environment, definition of VOC varies among different regulatory systems. The Canadian Environmental Protection Act (CEPA) defines VOCs based on their impact on air quality as "carbon-containing gases and vapors such as gasoline fumes and solvents excluding carbon dioxide, carbon monoxide, methane, and chlorofluorocarbons"(Environment Canada). The United State Environmental Protection Agency (USEPA) has another definition for VOC as "any compound of carbon excluding carbon monoxide, carbon dioxide, carbonic acid, metallic carbides or carbonates, and ammonium carbonate, which participate in atmospheric photochemical reaction (US Environmental Protection Agency 2009).

The main emission sources of VOC can be divided into two main categories: biogenic source and anthropogenic sources. Woods, crops, oceans, and volcanos are the major biogenic sources of VOC emission (Guenther et al. 1995). In addition to the oil and gas industry, which are the main anthropogenic sources of volatile organic compounds, painting, printing, adhesive, coating and pharmaceutical industries generate large amounts of VOCs (1768 kilotons in Canada during 2012) (Golovoy et al. 1981, Lu et al. 2004, Yu et al. 2007, Ramos et al. 2010, Kim 2011, Environment Canada 2014). Solvents and painting from

industries have quite large contributions in VOC emission (323 kilotons in Canada during 2012) (Environment Canada 2014). Painting operation in automotive manufacturing industry is one of the sections that generates large amount of VOC (Golovoy et al. 1981, Kim 2011). Based on previous studies, 6.58 kg of VOCs is used as painting materials per vehicle in a typical automotive plant in North America (Kim 2011).

It is essential to control VOC emissions to meet the environmental regulations because of their effect on human health and environment (Ramos et al. 2010). Some VOCs are toxic and can cause serious problem for human health such as headache, throat irritations, nausea, dizziness, memory loss, and damage to liver, central nervous system and lungs (Leslie 2000, Kampa et al. 2008, US Environmental Protection Agency 2013). Some of them are carcinogens, mutagens even at very low concentrations (as low as 0.25 ppm) (Strauss et al. 1984, Pariselli et al. 2009). The VOCs can form photochemical smog at the tropospheric level of atmosphere which leads to respiratory problem for human and damage to building and vegetation (De Nevers 2000, Das et al. 2004).

Methods used for VOC removal for indoor and outdoor air quality control systems are categorized into two main categories of destructive methods and non-destructive methods (Khan et al. 2000, Berenjian et al. 2012). Destructive methods include thermal oxidation, catalytic oxidation, and biofiltration (Khan et al. 2000, Berenjian et al. 2012). Destructive methods are used usually when solvent doesn't worth recovery or disposal of solvent is a concern for the process (Berenjian et al. 2012). Thermal oxidation has high energy recovery (Kim 2011)

but it is not suitable for low VOC concentrations and needs a product treatment process before releasing the product to the atmosphere (Khan et al. 2000). Catalytic oxidation is a method with moderate energy recovery but its disadvantage is poisoning of catalyst (Khan et al. 2000). Biofiltration is a suitable method for low concentration VOC streams and allows energy recovery (Kim 2011) but its application is limited because of its low removal efficiency and slow process (Khan et al. 2000). Another issue with biofiltration is that it can't tolerate high fluctuation of concentration in the process (Sullivan et al. 2004a, Hashisho et al. 2008).

Non-destructive or recovery methods are used when VOCs have recovery value and need to be collected for recovery and reuse. These methods include absorption, adsorption, condensation, and membrane separation (Khan et al. 2000). Recovery efficiency for condensation is satisfactory but this method is not cost effective for low concentration, has low removal efficiency, and is only applicable for removal of VOCs with low boiling point (<30 °C) (Khan et al. 2000, Hashisho et al. 2008, Mohan et al. 2009). Absorption is a method to remove VOC from a gas stream using a liquid in which the VOC is soluble (Schnelle et al. 2001). This method is already developed for removal of SO_2 from combustion gas and H_2S from natural gas. However, the application of absorption is limited because this method requires distillation or extraction after removal of VOC that increases the cost of the process (Khan et al. 2000).

Adsorption is perhaps the most common method for controlling VOC emissions because it has low costs, is highly efficient, allows for adsorbate

recovery, allows energy recovery by using fuel cell, and can control low concentrations (ppb level) (Sullivan et al. 2004a, Wherrett et al. 2004, Dabrowski et al. 2005, Mallouk et al. 2010, Ramos et al. 2010, Sidheswaran 2012). In addition, high inlet concentration, fluctuation, and VOCs boiling point aren't any limitation for this method (Khan et al. 2000, Hashisho et al. 2008). Because of the advantages of the adsorption process, this method was chosen as the VOC removal method in this research.

Adsorption depends on the structure and composition of adsorbent's surface. Therefore, adsorbent's surface area, pore size distribution, and surface functional groups are the most important parameters of an adsorbent in adsorption process (Gregg et al. 1991). Adsorbents can be categorized as carbonaceous adsorbents (activated carbon) and non- carbonaceous adsorbents. Non-carbonaceous adsorbents include activated alumina, silica gel, zeolites and polymeric adsorbents. Carbonaceous adsorbents are made by pyrolyzing organic materials (e.g. nutshell, coal, or synthetic polymers) to remove their hydrogen and oxygen contents then activating using steam or CO_2 to create porous structure and increase surface area and concentration of functional groups (Subrenat et al. 2001). Activated carbon is hydrophobic and organophilic in nature because carbon is non-polar (Ruthven 1984). This fact and its high surface area and micropore volume make activated carbon a suitable adsorbent for our study.

Activated carbon fiber cloth (ACFC) is an ash free activated carbon that provides high surface area, micropore volume, and adsorption capacity, making it an effective VOC adsorbent (Ramos et al. 2010). ACFC's internal micropores are

connected to its external surface area, helping to decrease mass and heat transfer limitations and pressure drop (Ramos et al. 2010). Higher mass and heat transfer rates improve adsorption/regeneration rate and decrease ignition threats inside the adsorption bed, respectively (Dombrowski et al. 2004). Activated carbon fiber cloth can be made from different precursor material such as novoloid, PAN, pitch, cellulose (Subrenat et al. 2001). ACFC used in this research was made from novoloid precursor (American Kynol). Figure 1-1 shows the manufacturing processes of novoloid-based ACFC.

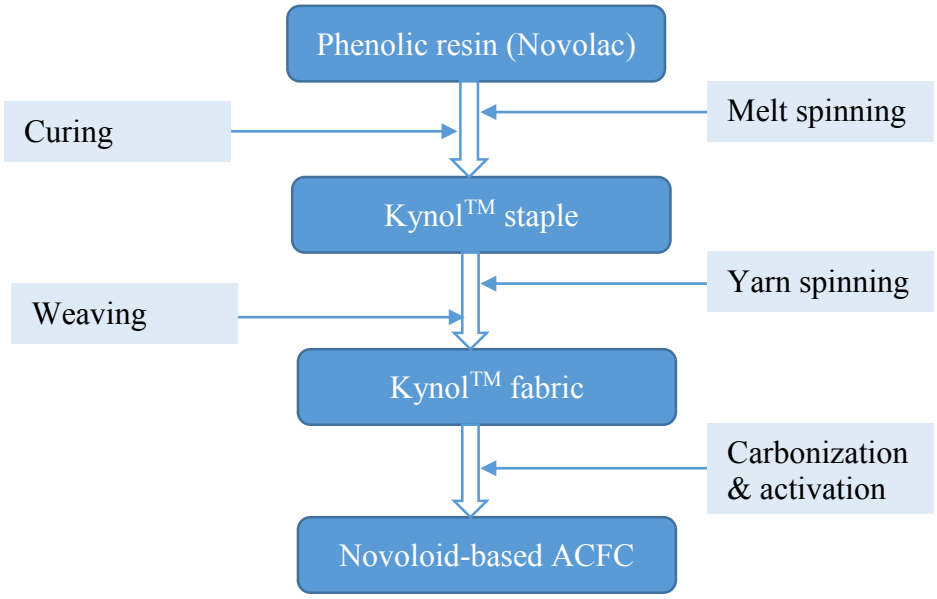

Figure 1-1. Manufacturing processes of novoloid-based ACFC

Novoloid fibers are first made by melt spinning of novolac resin. In melt spinning, heat is used to melt the fiber polymer to a material suitable for extrusion. The melt-spun fiber then is cured with an acidic solution of formaldehyde to turn the novolac resin into a cross-linked polymer (Hayes 1981).

One-step of carbonisation and activation is the last step to form novoloid-based ACFC. Figure 1-2 illustrates the SEM image of a novoloid-based ACFC (ACFC-10) and visual form of ACFC sample before the experiment.

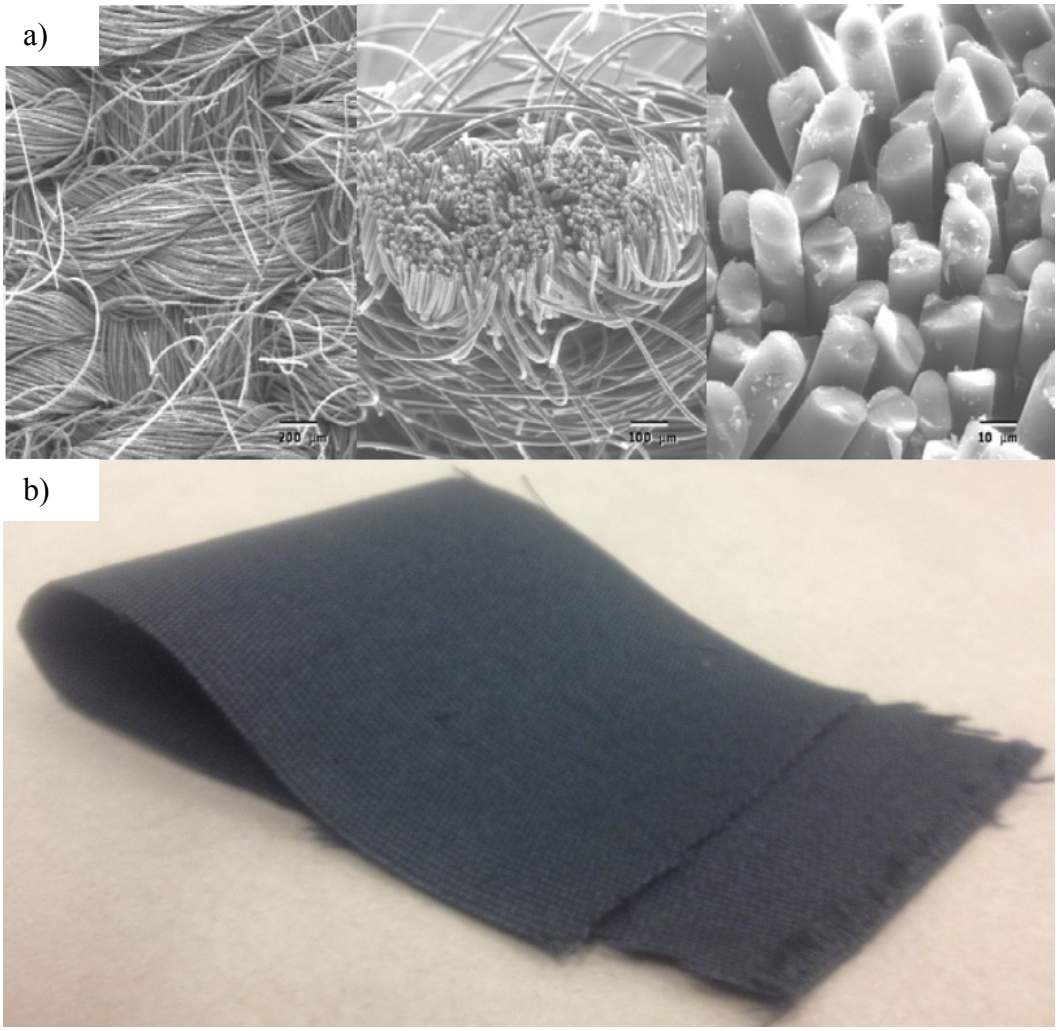

Figure 1-2. ACFC sample: a) SEM image of virgin sample (Lo 2000), b) picture of the sample before experiment

ACFC is more electrically conductive than many other activated carbons, making it a suitable material for electrical swing adsorption (ESA), where resistive heating causes VOC desorption (Dombrowski et al. 2004, Mallouk et al.

2010). ESA is an efficient heating method, providing higher heating rates and lower carrier gas consumption during regeneration (Sullivan et al. 2004a, Sullivan et al. 2004b, Mallouk et al. 2010). Heating rate of the ACFC is independent of heat/mass transfer rates of carrier gas and energy is applied directly to the adsorbent. Additionally, unlike steam regeneration, ESA does not require condensate separation and drying after regeneration, and unlike hot gas regeneration, adsorbent heating rate is independent of gas flow rate, decreasing carrier gas consumption and increasing effluent maximum concentration (Sullivan et al. 2004b).

Heel build-up or, irreversible adsorption, is the unwanted accumulation of adsorbate on an adsorbent surface or in adsorbent pores after regeneration under specified conditions (temperature and time). It is a challenge associated with using activated carbon for VOC adsorption because heel decreases the adsorbent's capacity and corresponding lifespan, increasing operation and maintenance costs. Established heel formation mechanisms include strong physical adsorption (Thakkar et al. 1987), chemical adsorption (Lowell et al. 1991, Ferro-Garcia et al. 1995, Ha et al. 2000, Lashaki et al. 2012), oligomerization (Grant et al. 1990, Vinitnantharat et al. 2001, Lu et al. 2004, Lu et al. 2007), and adsorbate decomposition (Ania et al. 2004, Ania et al. 2005, Caliskan et al. 2012).

Physical interactions, such as van der Waals' forces and other weak interactions between adsorbate and adsorbent are responsible for physisorption (Yonge et al. 1985, Lowell et al. 1991, Khan et al. 2000, Aktas et al. 2006). Because of the low heat of adsorption (typically 1-2 kcal/mol) associated with

these weak interactions, physisorption is generally reversible (Ruthven 1984, Khan et al. 2000, Bhushan 2013). According to Popescu *et al*., the heat of adsorption of a molecule physically adsorbed is similar to or slightly higher than its heat of vaporization (Popescu et al. 2003). In chemical adsorption, or chemisorption, adsorbate and adsorbent are connected by chemical bonds, typically covalent bonds (Yonge et al. 1985, Lowell et al. 1991, De Jonge et al. 1996, Ha et al. 2000, Aktas et al. 2006). Therefore, the heat of adsorption is much higher than physisorption and close to the energy of chemical bonds (10-100 kcal/mol) (Lowell et al. 1991, Bhushan 2013).

Oxidative coupling or, oligomerization, is the polymerization of organic compounds in the presence of oxygen (Soto et al. , De Jonge et al. 1996, Vinitnantharat et al. 2001). Recent studies confirm that oxidative coupling is the main mechanism for irreversible adsorption of aqueous phenolic compounds in presence of oxygen (Vidic et al. 1991, Vidic et al. 1993, Vidic et al. 1997). In oxidative coupling, a phenol molecule loses one hydrogen atom, forming a phenoxy radical that will react with other phenoxy radicals, even at room temperature, on an activated carbon surface that acts as a catalyst (Vidic et al. 1993). Adsorbate decomposition depends mostly on the regeneration conditions used for desorption and can occur when aromatic hydrocarbons are exposed to the high temperatures (Chang et al. 1998). Adsorbate decomposition causes carbonaceous species to stick inside the adsorbent's pores, block the micropores, and decrease adsorption capacity (Ania et al. 2004, Ania et al. 2005, Caliskan et al. 2012).

1-2. Objectives

The goal of this research is to identify the reason and mechanism for heel formation resulting from the adsorption and desorption of organic vapors on ACFC. 1,2,4-trimethylbenzene (TMB) was used as the adsorbate and activated carbon fiber cloth (ACFC) was used as the adsorbent. Therefore, the main objectives of this research can be describe as:

1. To investigate the effect of regeneration temperature on the adsorption capacity and heel build-up during adsorption of TMB on three activated carbon fiber cloth samples with different surface areas and pore volumes
2. To explore the effect of regeneration heating rate and regeneration flow rate on heel build-up and adsorption capacity during adsorption of a volatile organic compound on ACFC.

A better understanding of heel build-up and the parameters enhancing it is useful to find effective ways to decrease this parameter and increase the lifetime of the adsorbent. Adsorbate decomposition is a justified concern when heating adsorbents for regeneration, but the limited number of references are inconclusive regarding the specific cause. Identifying the adsorbents and adsorbates properties and the regeneration conditions that favor adsorbate decomposition is essential, but has not yet been described. Result of this research provides information to decrease the magnitude of heel build-up. As a result, related industry can save a lot in adsorbent consumption, disposal of spent adsorbent and labour cost.

Moreover, this research can cover some of the knowledge gaps in the adsorption/regeneration of VOC from gas stream onto ACFC. Results of this research can be also used for designing an effective abatement system for capturing VOCs from polluted air using ACFC.

1-3. Thesis Outline

This thesis consists of four chapters which will contribute to fulfill the main goal of this research. Chapter 1 provides an introduction about background, objective, and significance of this work. The second chapter is focused on heel formation during VOC desorption from activated carbon fiber cloth using resistive heating method. Chapter 3 explains the effect of regeneration flow rate and heating rate on heel formation during desorption of 1,2,4-trimethylbenzene from activated carbon fiber cloth. The second and third chapter also reviews previous works conducted in the area of this research. The conclusion derived from this research and recommendation for future work are presented in the fourth chapter.

1-4. References

Aktas, O. and F. CeCen (2006). "Effect of type of carbon activation on adsorption and its reversibility." Journal of Chemical Technology & Biotechnology **81**(1): 94-101.

Ania, C. O., J. A. Menendez, J. B. Parra and J. J. Pis (2004). "Microwave-induced regeneration of activated carbons polluted with phenol. A comparison with conventional thermal regeneration." Carbon **42**(7): 1383-1387.

Ania, C. O., J. B. Parra, J. A. Menendez and J. J. Pis (2005). "Effect of microwave and conventional regeneration on the microporous and mesoporous network and on the adsorptive capacity of activated carbons." Microporous and Mesoporous Materials **85**(1–2): 7-15.

Berenjian, A., N. Chan and H. J. Malmiri (2012). "Volatile organic compounds removal methods: A review." American Journal of Biochemistry and Biotechnology **8**(4): 220-229.

Bhushan, B. (2013). Introduction to Tribology, Wiley.

Caliskan, E., J. M. Bermudez, J. B. Parra, J. A. Menendez, M. Mahramanlıoğlu and C. O. Ania (2012). "Low temperature regeneration of activated carbons using microwaves: Revising conventional wisdom." Journal of Environmental Management **102**(0): 134-140.

Chang, P. H. and S. EseI (1998). Effect of carbon surface on thermal decomposition of hydrocarbons. ABSTRACTS OF PAPERS OF THE AMERICAN CHEMICAL SOCIETY, AMER CHEMICAL SOC 1155 16TH ST, NW, WASHINGTON, DC 20036 USA.

Dabrowski, A., P. Podkoscielny, Z. Hubicki and M. Barczak (2005). "Adsorption of phenolic compounds by activated carbon: a critical review." Chemosphere **58**(8): 1049-1070.

Das, D., V. Gaur and N. Verma (2004). "Removal of volatile organic compound by activated carbon fiber." Carbon **42**(14): 2949-2962.

De Jonge, R. J., A. M. Breure and J. G. van Andel (1996). "Reversibility of adsorption of aromatic compounds onto powdered activated carbon (PAC)." Water Research **30**(4): 883-892.

De Nevers, N. (2000). Air Pollution Control Engineering: Internationl Edition, Mc-Graw-Hill.

Dombrowski, K., C. Lehmann, P. Sullivan, D. Ramirez, M. Rood and K. Hay (2004). "Organic vapor recovery and energy efficiency during electric regeneration of an activated carbon fiber cloth adsorber." Journal of Environmental Engineering **130**(3): 268-275.

Environment Canada (2013-07-17). "Volatile Organic Compounds (VOCs)." from https://www.ec.gc.ca/air/default.asp?lang=En&n=15B9B65A-1.

Environment Canada (2014). "Volatile Organic Compound Emissions." Retrieved 12 Jan, 2014, from http://www.ec.gc.ca/indicateurs-indicators/default.asp?lang=en&n=64B9E95D-1

Ferro-Garcia, M. A., J. P. Joly, J. Rivera-Utrilla and C. Moreno-Castilla (1995). "Thermal desorption of chlorophenols from activated carbons with different porosity." Langmuir **11**(7): 2648-2651.

Golovoy, A. and J. Braslaw (1981). "Adsorption of automotive paint solvents on activated carbon: I. Equilibrium adsorption of single vapors." Journal of the Air Pollution Control Association **31**(8): 861-865.

Grant, T. M. and C. J. King (1990). "Mechanism of irreversible adsorption of phenolic compounds by activated carbons." Industrial & Engineering Chemistry Research **29**(2): 264-271.

Gregg, S. J. and K. S. W. Sing (1991). Adsorption, Surface area, and Porosity, Academic Press.

Guenther, A., C. N. Hewitt, D. Erickson, R. Fall, C. Geron, T. Graedel, P. Harley, L. Klinger, M. Lerdau and W. McKay (1995). "A global model of natural volatile organic compound emissions." Journal of Geophysical Research: Atmospheres **100**(D5): 8873-8892.

Ha, S. R. and S. Vinitnantharat (2000). "Competitive removal of phenol and 2,4-dichlorophenol in biological activated carbon system." Environmental Technology **21**(4): 387-396.

Hashisho, Z., H. Emamipour, M. J. Rood, K. J. Hay, B. J. Kim and D. Thurston (2008). "Concomitant adsorption and desorption of organic vapor in dry and humid air streams using microwave and direct electrothermal swing adsorption." Environmental Science Technolology **42**(24): 9317-9322.

Hayes, J.S. (1981). Novoloid Fibers. In Kirk-Othmer Encyclopedia of Chemical Technology, John Wiley and Sons, 125-138.

Kampa, M. and E. Castanas (2008). "Human health effects of air pollution." Environmental Pollution **151**(2): 362-367.

Kennes, C. and M. C. Veiga (2013). Air Pollution Prevention and Control: Bioreactors and Bioenergy, Wiley.

Khan, F. I. and A. Kr. Ghoshal (2000). "Removal of volatile organic compounds from polluted air." Journal of Loss Prevention in the Process Industries **13**(6): 527-545.

Kim, B. R. (2011). "VOC emissions from automotive painting and their control: A review." Environmental Engineering Research **16**(1): 1-9.

Lashaki, M., M. Fayaz, H. Wang, Z. Hashisho, J. H. Philips, J. E. Anderson and M. Nichols (2012). "Effect of adsorption and regeneration temperature on irreversible adsorption of organic vapors on beaded activated carbon." Environmental Science & Technology **46**(7): 4083-4090.

Leslie, G. B. (2000). "Review : Health risks from indoor air pollutants: public alarm and toxicological reality." Indoor and Built Environment **9**(1): 5-16.

Lo, S. Y. (2000). "Characterization of the chemical, physical, thermal and electrical properties of a series of activated carbon fiber cloths", University of Illinois at Urbana–Champaign. MSc.

Lowell, S. and J. E. Shields (1991). Powder Surface Area and Porosity, Springer.

Lu, Q. and G. A. Sorial (2004). "Adsorption of phenolics on activated carbon–impact of pore size and molecular oxygen." Chemosphere **55**(5): 671-679.

Lu, Q. and G. A. Sorial (2007). "The effect of functional groups on oligomerization of phenolics on activated carbon." Journal of Hazardous Materials **148**(1–2): 436-445.

Mallouk, K. E., D. L. Johnsen and M. J. Rood (2010). "Capture and recovery of isobutane by electrothermal swing adsorption with post-desorption liquefaction." Environmental Science & Technology **44**(18): 7070-7075.

Mohan, N., G. K. Kannan, S. Upendra, R. Subha and N. S. Kumar (2009). "Breakthrough of toluene vapours in granular activated carbon filled packed bed reactor." Journal of Hazardous Materials **168**(2–3): 777-781.

Pariselli, F., M. G. Sacco, J. Ponti and D. Rembges (2009). "Effects of toluene and benzene air mixtures on human lung cells (A549)." Experimental and Toxicologic Pathology **61**(4): 381-386.

Popescu, M., J. P. Joly, J. Carre and C. Danatoiu (2003). "Dynamical adsorption and temperature-programmed desorption of VOCs (toluene, butyl acetate and butanol) on activated carbons." Carbon **41**(4): 739-748.

Ramos, M. E., P. R. Bonelli, A. L. Cukierman, M. M. L. Ribeiro Carrott and P. J. M. Carrott (2010). "Adsorption of volatile organic compounds onto activated carbon cloths derived from a novel regenerated cellulosic precursor." Journal of Hazardous Materials **177**(1–3): 175-182.

Ruthven, D. M. (1984). Principles of Adsorption and Adsorption Processes, Wiley.

Schnelle, K. B. and C. A. Brown (2001). Air Pollution Control Technology Handbook, Taylor & Francis.

Sidheswaran, M. (2012). "Energy Efficient Indoor VOC Air Cleaning with Activated Carbon Fiber (ACF) Filters."

Soto, M. L., A. Moure, H. Dominguez and J. C. Parajo "Recovery, concentration and purification of phenolic compounds by adsorption: A review." Journal of Food Engineering **105**(1): 1-27.

Strauss, W. and S. J. Mainwaring (1984). Air Pollution, Edward Arnold.

Subrenat, A., J. N. Baléo, P. Le Cloirec and P. E. Blanc (2001). "Electrical behaviour of activated carbon cloth heated by the joule effect: desorption application." Carbon **39**(5): 707-716.

Sullivan, P., M. Rood, K. Dombrowski and K. Hay (2004). "Capture of organic vapors using adsorption and electrothermal regeneration." Journal of Environmental Engineering **130**(3): 258-267.

Sullivan, P. D., M. J. Rood, G. Grevillot, J. D. Wander and K. J. Hay (2004). "Activated carbon fiber cloth electrothermal swing adsorption system." Environmental Science & Technology **38**(18): 4865-4877.

Thakkar, S. and M. Manes (1987). "Adsorptive displacement analysis of many-component priority pollutants on activated carbon." Environmental Science Technology **21**(6): 546-549.

US Environmental Protection Agency (2009, 6/11/2013). "Definition of Volatile Organic Compounds (VOC)." from http://www.epa.gov/ttn/naaqs/ozone/ozonetech/def_voc.htm.

US Environmental Protection Agency (2013, 7/17/2014). "National Emissions Inventory (NEI) Air Pollutant Emissions Trends Data." from http://www.epa.gov/ttn/chief/trends/index.html.

Vidic, R. D. and M. T. Suidan (1991). "Role of dissolved oxygen on the adsorptive capacity of activated carbon for synthetic and natural organic matter." Environmental Science & Technology **25**(9): 1612-1618.

Vidic, R. D., M. T. Suidan and R. C. Brenner (1993). "Oxidative coupling of phenols on activated carbon: impact on adsorption equilibrium." Environmental Science & Technology **27**(10): 2079-2085.

Vidic, R. D., C. H. Tessmer and L. J. Uranowski (1997). "Impact of surface properties of activated carbons on oxidative coupling of phenolic compounds." Carbon **35**(9): 1349-1359.

Vinitnantharat, S., A. Baral, Y. Ishibashi and S. R. Ha (2001). "Quantitative bioregeneration of granular activated carbon loaded with phenol and 2,4-dichlorophenol." Environmental Technology **22**(3): 339-344.

Wherrett, M. R. and P. A. Ryan (2004). "VOC emissions from industrial painting processes as a source of fuel cell energy." Metal Finishing **102**(10): 23-29.

Yonge, D. R., T. M. Keinath, K. Poznanska and Z. P. Jiang (1985). "Single-solute irreversible adsorption on granular activated carbon." Environmental Science & Technology **19**(8): 690-694.

Yu, F. D., L. Luo and G. Grevillot (2007). "Electrothermal swing adsorption of toluene on an activated carbon monolith: Experiments and parametric theoretical study." Chemical Engineering and Processing: Process Intensification **46**(1): 70-81.

CHAPTER 2 HEEL FORMATION DURING VOC DESORPTION FROM ACTIVATED CARBON FIBER CLOTH USING RESISTIVE HEATING

A version of this chapter will be submitted for publication. Reproduced with permission from Saeid Niknaddaf, John D. Atkinson, Pooya Shariaty, Masoud Jahandar Lashaki, Zaher Hashisho, John H. Philips, James E. Anderson, Mark Nichols

2-1. Introduction

Automotive painting booths are the main source of volatile organic compounds (VOCs) in automotive manufacturing industries (Golovoy et al. 1981, Kim 2011). About 6.58 kg of VOCs per vehicle is used as paint solvents during automotive manufacturing in a typical Ford plant in North America (Kim 2011). Emissions from painting and coating operations include aromatic hydrocarbons, esters, ketones, alcohols, and other organic compounds, with a wide range of molecular weights and boiling points (< 240 °C).(Golovoy et al. 1981, Kim 2011, Kennes et al. 2013) Adsorption is a common control technology for these emissions because it is low cost and efficient, allows for adsorbate recovery, and can control low VOC concentrations (ppb level) (Sullivan et al. 2004a, Dabrowski et al. 2005, Mallouk et al. 2010, Ramos et al. 2010, Lashaki et al. 2012, Sidheswaran 2012).

Activated carbon fiber cloth (ACFC) is an ash-free, porous carbon that provides high surface area, micropore volume, and adsorption capacity, making it an effective VOC adsorbent (Hashisho et al. 2009, Ramos et al. 2010). ACFC's internal micropores are connected to its external surface area, decreasing mass and heat transfer limitations (Mangun et al. 1999, Ramos et al. 2010). Higher mass and heat transfer rates improve adsorption/regeneration rates and decrease the risk of ignition inside the adsorption bed, respectively (Dombrowski et al. 2004). ACFC is more electrically conductive than other activated carbons because it consists of continuous fibers, making it a suitable material for electrothermal swing adsorption (ESA) (Lordgooei et al. 1996, Subrenat et al. 2001,

Dombrowski et al. 2004, Hashisho et al. 2008, Mallouk et al. 2010). ESA uses resistive heating to provide higher heating rates than more traditional conductive heating and steam regeneration methods, and it consumes less purge gas (Sullivan et al. 2004a, Sullivan et al. 2004b, Mallouk et al. 2010). Additionally, unlike steam regeneration, ESA does not require condensate separation and drying after regeneration, and unlike hot gas regeneration, the adsorbent heating rate is independent of carrier gas flow rate, decreasing gas consumption (Sullivan et al. 2004b).

Heel build-up is the unwanted accumulation of adsorbate on an adsorbent surface or in adsorbent pores after regeneration under specified conditions (temperature and time). It is a challenge associated with using activated carbon for VOC adsorption because heel decreases the adsorbent's capacity and corresponding lifespan, increasing operation and maintenance costs. Established heel formation mechanisms include strong physical adsorption (Thakkar et al. 1987), chemical adsorption (Lowell et al. 1991, Ferro-Garcia et al. 1995, Ha et al. 2000, Lashaki et al. 2012), oligomerization (Grant et al. 1990, Vinitnantharat et al. 2001, Lu et al. 2004, Lu et al. 2007), and adsorbate decomposition (Ania et al. 2004, Ania et al. 2005, Caliskan et al. 2012). Adsorbate decomposition depends most prominently on the regeneration conditions used for desorption. Change *et al*. confirmed that thermal decomposition of aromatic hydrocarbons can occur when they are exposed to high temperatures (450 °C) (Chang et al. 1998). Ania *et al*. found that pore blockage attributed to high temperature decomposition of adsorbed phenols occurs during microwave regeneration of activated carbons at

850 °C (Ania et al. 2004). Pore blockage in a powder activated carbon was similarly attributed to adsorbate (promethazine hydrochloride) decomposition during moderate temperature microwave regeneration (300 °C – 500 °C) (Caliskan et al. 2012).

Adsorbate decomposition is a justified concern when heating adsorbents for regeneration, but the limited number of references are inconclusive regarding the specific cause. For example, while activated carbon fiber cloth is a widely studied VOC adsorbent and resistive heating is extensively tested carbon regeneration method, there has been no description of heel formation associated with adsorbate decomposition during their use. Identifying the adsorbents and adsorbates properties and the regeneration conditions that favor adsorbate decomposition is essential, but has not yet been described. The main objective of this research, therefore, is to identify the reason and mechanism for heel formation resulting from the adsorption and desorption of organic vapors on ACFC.

2-2. Materials and Methods

2-2-1. Adsorbent and Adsorbate

The adsorbent was ACFC prepared from phenol-formaldehyde resin precursor (Nippon Kynol Company). Three samples (ACC-5092-10 (ACFC10), ACC-5092-15 (ACFC15), and ACC-5092-20 (ACFC20)) with different levels of activation, corresponding to different pore size distributions, were used. Prior to use, all ACFCs underwent 2 h of heat treatment at 288 °C or 400 °C, depending

on the selected regeneration conditions, to remove adsorbed water vapor and volatile organic compounds. 1, 2, 4-trimethylbenzene (TMB, 98%, Acros Organics) and acetone (99.8%, Fisher Scientific) were the adsorbates. TMB is bulky (kinetic diameter = 0.61 nm (Klinowski et al. 1989)) with a high boiling point (171 °C) while acetone is small (kinetic diameter = 0.44 nm (Jahandar Lashaki et al. 2012)) with a lower boiling point (56 °C).

2-2-2. Experimental Set-Up and Methods

The experimental set-up includes an adsorption/regeneration cartridge, an adsorbate generation system, a gas detection system, a heat application module, and a data acquisition and control system (DAC) (Figure 2-1). The cartridge consisted of a 3-layer annular ACFC cartridge (1.65 cm inner diameter, 10 cm length) attached to two stainless steel electrode tubes (1.65 cm outer diameter). Because the ACFC samples have different areal densities, different masses were required to prepare the 3-layer cartridges (5.5 g, 4.5 g, and 3.5 g for ACFC10, ACFC15, and ACFC20, respectively). The prepared cartridge was mounted inside a quartz tube to prevent exposure to ambient air (7.3 cm inner diameter, 40 cm length).

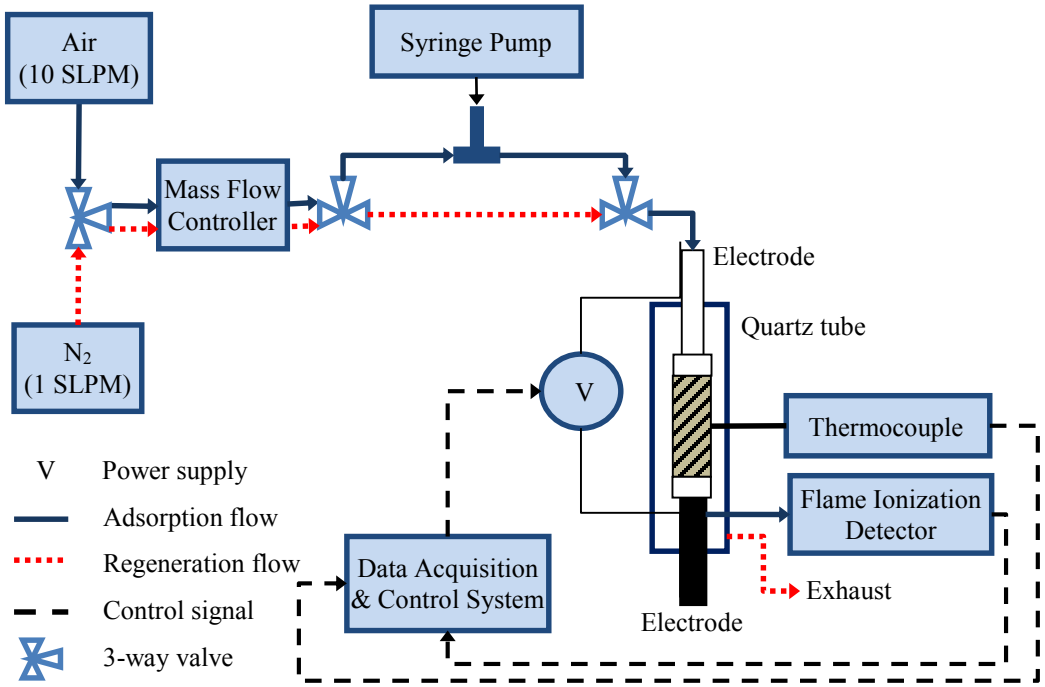

Figure 2-1. Schematic diagram of the adsorption/regeneration set-up

The inlet adsorbate concentration was 500 ppm_v for all experiments. The adsorbate generation system used a syringe pump (New Era Inc., NE-300) to inject liquid organic compound into a dry air stream maintained at10 Standard Liter Per Minute (SLPM) (standard conditions are 25 °C and 1 atm) with a mass flow controller (Alicat Scientific). Liquid injection rates were determined using the ideal gas law. VOC concentrations were measured using a flame ionization detector (FID, Baseline-Mocon Inc., series 9000). The VOC concentration in the adsorption tube's outlet stream was measured continuously during adsorption (2 min sampling frequency), and the FID was calibrated before each adsorption test using the same gas generation system.

The heat application module for adsorbent regeneration included a silicon-controlled rectifier (SCR) to apply voltage to both sides of the ACFC cartridge. A 1.6 mm outer diameter, ungrounded, type K thermocouple (Omega) was used to measure the temperature at the center of the ACFC cartridge during adsorption and regeneration. The DAC system consisted of a LabVIEW program (National Instruments) and a data logger (National Instruments, Compact DAQ) equipped with analog input/output modules. The data logger was interfaced to the FID and thermocouple to record outlet VOC concentration during adsorption and temperature during adsorption and regeneration. A proportional-integral-derivative control algorithm and a silicon-controlled rectifier were used to control the voltage applied to the cartridge to achieve and maintain the set-point temperature.

After FID calibration, the gas stream containing organic vapor was introduced to the adsorption tube, and outlet VOC concentration measurement began, generating a breakthrough curve. Adsorption was done at 25 °C and continued until the ACFC cartridge was saturated (approximately 2 h). Adsorption capacity was calculated as follows:

$$Amount\ adsorbed\ (\text{wt}\%) = \frac{\text{Cartridge weight after adsorption} - \text{Cartridge weight before adsorption}}{\text{Weight of virgin ACFC}} \text{X}100$$

Regeneration was completed by heating the ACFC cartridge at 288 °C or 400 °C for 100 min and then cooling for 30 min while purging with 1 SLPM N_2. When cool (25 °C), the cartridge was again weighed. The difference in the

cartridge mass before adsorption and after regeneration is the amount of heel build-up during that cycle. Cumulative heel after five adsorption/regeneration cycles is described as:

$$Cumulative\ heel\ (\text{wt}\%) = \frac{\text{Weight after } 5^{th} \text{ regeneration cycle } - \text{Weight before } 1^{\text{st}} \text{ adsorption cycle}}{\text{Weight of virgin ACFC}} \text{X100}$$

2-2-3. Micropore Surface Analysis

Pore size distribution and BET surface area were obtained using a micropore surface analysis system (Autosorb iQ2MP, Quantachrome) with N_2 ($10^{-7} < P/P_0 < 1$) adsorption at -196 °C. 30 – 50 mg of ACFC from the middle of outer layer was cut into pieces (2 mm × 2 mm), added to a 6 mm cell, and degassed at 150 °C for 5 h to remove moisture. BET surface area and micropore volume were obtained using relative pressure ranges of 0.01 – 0.07 and 0.2 – 0.4, respectively. The V-t model was used to calculate micropore volume. Mesopore volume and surface area were obtained by subtracting the relevant micropore values from the total pore values. Pore size distributions were obtained using the density functional theory (DFT) model for slit-shaped pores.

2-2-4. Thermogravimetric Analysis

The temperature stability of used and unused ACFCs was assessed using thermogravimetric and derivative thermogravimetric analyses (TGA/DTG, Mettler Toledo TGA/DSC 1). Each run included a temperature ramp from 25 °C to 100 °C (10 °C/min), isothermal heating at 100 °C for 15 min, and then a second

temperature ramp from 100 °C to 900 °C (5 °C/min). 50 ml/min N_2 purged desorbed species.

2-3. Results & Discussion

2-3-1. Adsorption/Regeneration:

The physical properties of virgin and tested ACFCs are included in Table 2-1. For the virgin samples, BET surface area, micropore volume, and total pore volume increased with activation level, from ACFC10 to ACFC20. All virgin ACFC samples had microporosity greater than 90%. These results are consistent with the literature (Lo 2000, Lu et al. 2004, Sullivan et al. 2004a, Lu et al. 2007, Sullivan et al. 2007).

Table 2-1. BET surface area, micropore volume, total pore volume, and microporosity of ACFC samples

	BET Surface Area (m^2/g)	Micropore Volume (cm^3/g)	Total Pore Volume (cm^3/g)	Microporosity
Virgin ACFC10	804	0.30	0.33	0.91
ACFC10, 5 cycles, 288 °C	605	0.24	0.27	0.90
ACFC10, 5 cycles, 400 °C	570	0.21	0.23	0.90
Virgin ACFC15	1215	0.45	0.47	0.96
ACFC15, 5 cycles, 288 °C	962	0.40	0.43	0.93
ACFC15, 5 cycles, 400 °C	813	0.29	0.33	0.88
Virgin ACFC20	1929	0.71	0.74	0.96
ACFC20, 5 cycles, 288 °C	1822	0.67	0.70	0.96
ACFC20, 5 cycles, 400 °C	1504	0.55	0.59	0.93

Adsorption breakthrough curves for TMB on all ACFCs and with regeneration temperatures of 288 °C and 400 °C are included in Figure 2-2. For regeneration at 288 °C, ACFC10's TMB breakthrough time ($t_{1\%}$, when the outlet concentration equals 1% of the inlet concentration) decreased by 55% after the first cycle and breakthrough occurred immediately ($t_{1\%}$ = 0 min) after the third cycle (Figure 2-2a), rendering the adsorbent useless. Adsorption/regeneration cycling has little effect on breakthrough time for ACFC15 and ACFC20 (less than 10% decrease after five cycles) when regenerated at 288 °C (Figure 2-2c and Figure 2-2e) indicating stable performance with continued use. Since the adsorbents have similar chemical properties (Lo 2000) and negligible ash content (Hashisho et al. 2009), it is concluded that differences in pore size distributions cause the distinctly different performance of ACFC10 compared to ACFC15 and ACFC20.

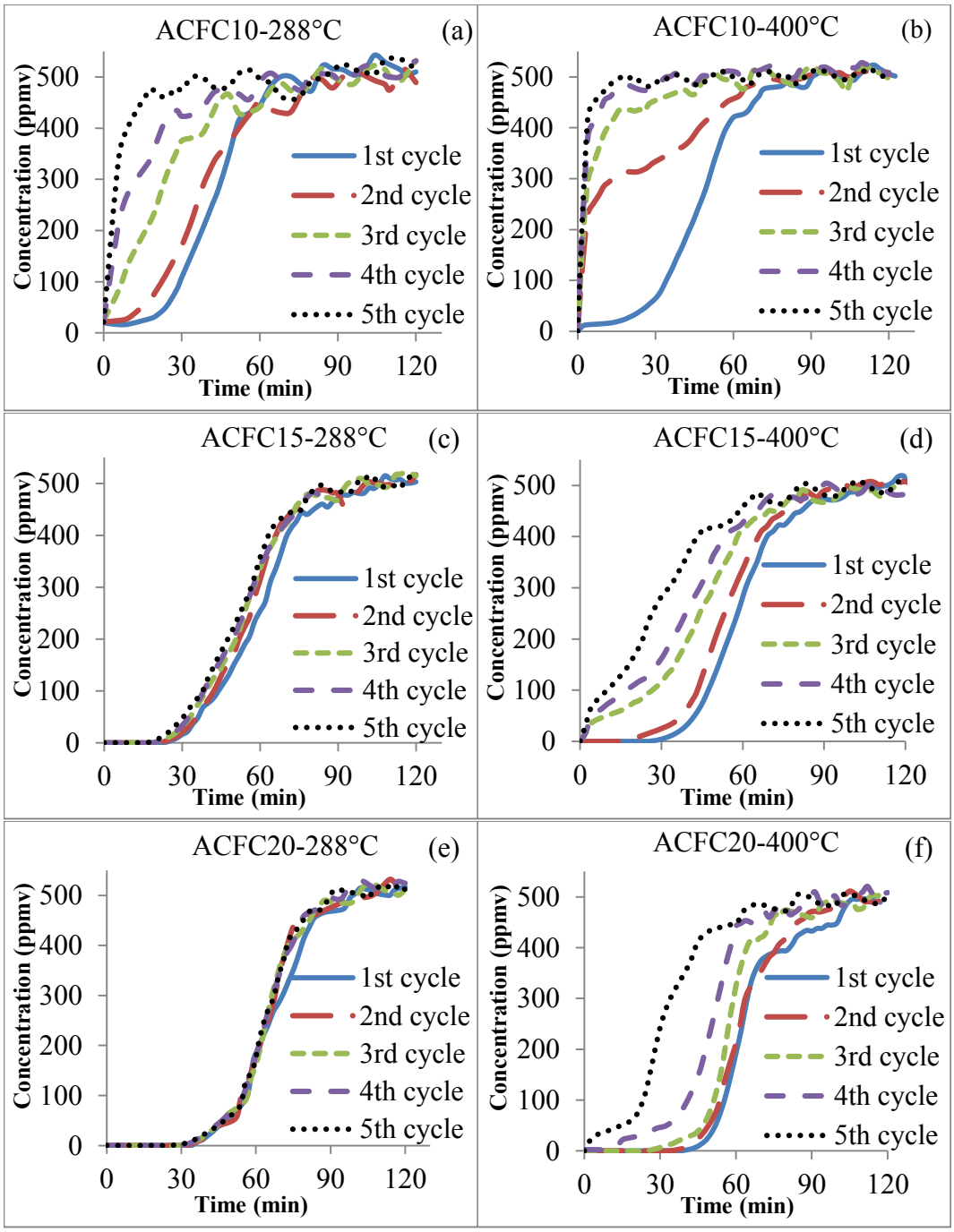

Figure 2-2. Adsorption breakthrough curves for 1,2,4-trimethylbenzene on ACFC samples: (a/b) ACFC10 regenerated at 288/400 °C, (c/d) ACFC15 regenerated at 288/400 °C, and (e/f) ACFC20 regenerated at 288/400 °C

Heel formation is often related to the difference between adsorbate boiling point and regeneration temperature – increasing regeneration temperature is expected to decrease heel and increase adsorption capacity during subsequent use (Fayaz et al. 2011, Lashaki et al. 2012). In this case, however, regeneration at a higher temperature (400 °C) decreased adsorption/regeneration performance for all ACFC samples (Figure 2-2 and 3). For ACFC10, breakthrough occurred immediately during the second cycle, compared to during the third cycle when regenerating at 288 °C (Figure 2-2b). ACFC15's TMB breakthrough time decreased by 44% after the first cycle and breakthrough occurred immediately during the third cycle (Figure 2-2d). ACFC20's breakthrough time decreased by 5%, 45%, and 75% during the second, third and fourth cycles, respectively. Immediate breakthrough ($t_{1\%}$ = 0 min) for ACFC20 occurred during the fifth cycle (Figure 2-2f). While differences remain between the three samples (i.e., in terms of performance, ACFC10 < ACFC15 < ACFC20), variability among samples is smaller than when regenerating at 288 °C, where ACFC10's performance is notably worse than the other materials.

TMB adsorption capacities for ACFCs regenerated at 288 °C or 400 °C are described in Figure 2-3. Virgin ACFC20 has the highest initial adsorption capacity because it has higher pore volume than ACFC15 and ACFC10 (Table 2-1). For ACFC15 and ACFC20 regenerated at 288 °C, adsorption capacity decreased by 8.8% and 5.4%, respectively, after five cycles. ACFC10's adsorption capacity decreased by 83.0%, from 20.7 wt% in the first cycle to 3.6

wt% in the fifth cycle. These results are consistent with the breakthrough curves for all ACFCs (Figure 2-2).

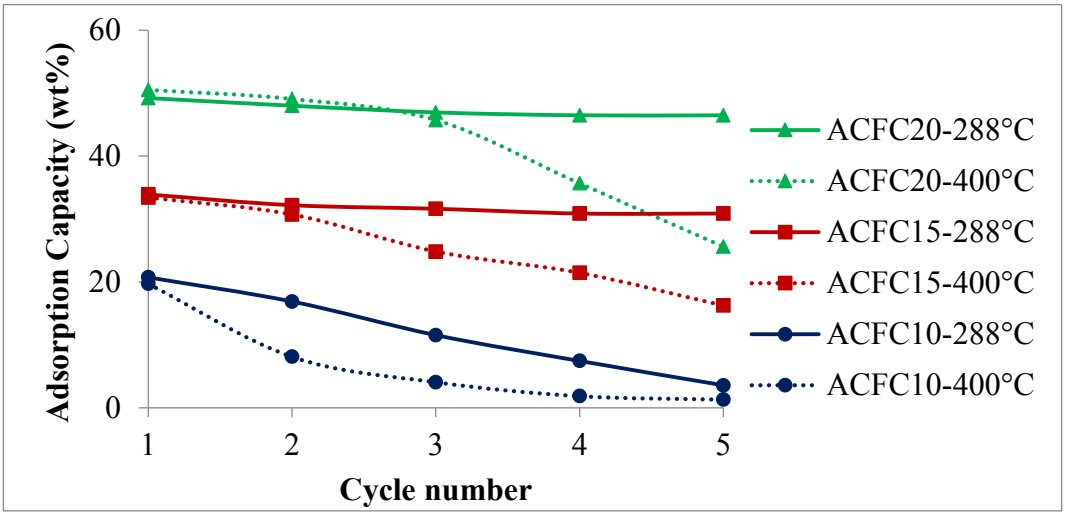

Figure 2-3. Adsorption capacity of ACFC samples after consecutive cycles of TMB adsorption with electrothermal regeneration. The numbers in the legend correspond to regeneration temperature

Adsorption capacity loss unexpectedly increased after increasing the regeneration temperature. Reduction in ACC10's adsorption capacity at 400 °C was 93% after 5 cycles, compared to 83% when regenerating at 288 °C. Adsorption capacity of ACC15 and ACC20 regenerated at 400 °C decreased by 51% and 50%, compared to a < 10% change when regenerating at 288 °C. Combined with the breakthrough curves in Figure 2-2, these results describe decreased performance for all ACFCs when regenerating at a higher temperature, which differs from most studies reported in the literature (Wang et al. 2009, Lashaki et al. 2012).

Five-cycle cumulative heel percentages for all ACFC samples are shown in Figure 2-4. For regeneration at 288 °C, heel values were between 3.5 and 4.5

wt%, with ACFC15 and ACFC20 having 25% higher cumulative heel than ACFC10. Heel after five adsorption/regeneration cycles at 400 °C increased for all samples to 3.8 wt%, 10.4 wt%, and 18.9 wt% for ACFC10, ACFC15, and ACFC20, respectively (Figure 2-4). Increasing heel with increasing ACFC activation level is attributed to variability in the micropore volume of ACFC samples (Table 2-1). High micropore volume increases desorbate diffusion resistance during regeneration, which has been shown to impact heel development (Carratala-Abril et al. 2010). This concept is described in more detail in discussions below.

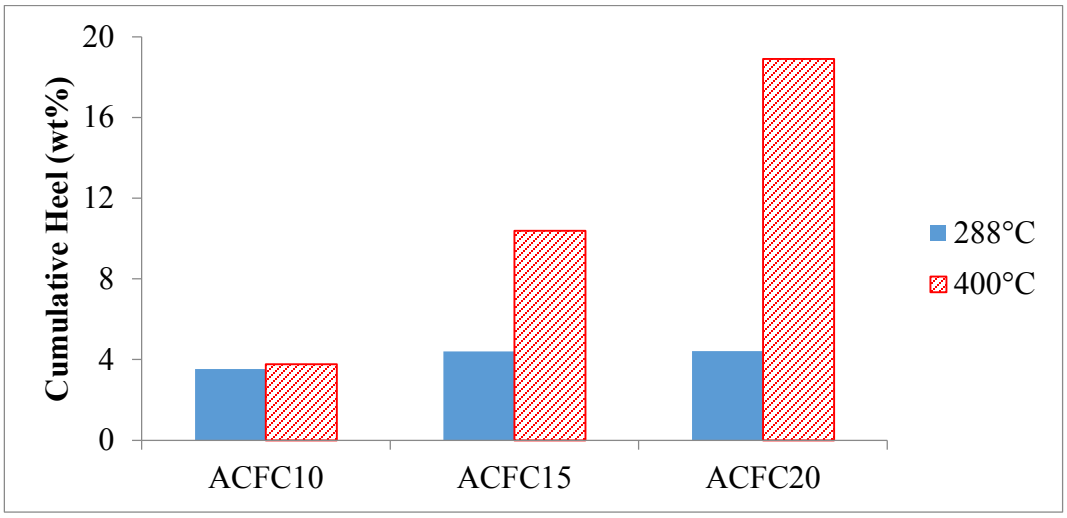

Figure 2-4. Cumulative heel percentage of ACFC samples after five cycles of adsorption with 1,2,4-trimethylbenzene and electrothermal regeneration.

After five cycles of TMB adsorption/regeneration, BET surface area, micropore volume, and total pore volume of all samples decreased (Table 2-1). This is consistent with the literature (Ania et al. 2004, Ania et al. 2005, Caliskan et al. 2012) and explained by heel formation causing partially or fully obstructed pores. After five cycles with regeneration at 288 °C, total pore volume of

ACFC10, ACFC15, and ACFC20 decreased by 18.2%, 8.5% and 5.4%, respectively. However, for regeneration at 400 °C, total pore volume of ACFC10, ACFC15 and ACFC20 decreased by 30.3%, 29.8% and 20.3%, respectively.

It is notable that when comparing Table 2-1 and Figure 2-3, ACFC10's total pore volume after five cycles with regeneration at 288 °C, decreased by 18.2%, while there was 82.6% reduction in adsorption capacity. In other words, the reduction in ACFC10's adsorption capacity for TMB was notably larger than for N_2, indicating partial pore obstruction that prevents accessibility to bulky molecules but permits accessibility to smaller ones. A similar phenomenon is notable for other samples, especially for the higher regeneration temperature (400 °C). To confirm this hypothesis, three cycles of TMB adsorption were followed by two cycles of acetone adsorption on ACFC10, with regeneration at 288 °C (Figure 2-5). The expectation is that because TMB is similar in size to the average ACFC pore widths (pore widths are 0.67 nm, 0.76 nm, and 0.86 nm for ACFC10, ACFC15, and ACFC20, respectively (Sullivan et al. 2007)) and acetone is smaller, these adsorbates can highlight the partial pore blockage that occurs during regeneration of the adsorbent loaded with TMB. Although breakthrough occurs immediately during the third cycle of TMB adsorption, suggesting loss of adsorption capacity due to pore blockage, subsequent acetone adsorption (4^{th} and 5^{th} cycles) is possible with breakthrough occurring after 10 min and stable adsorption capacities between cycles. This supports the hypothesis of partial pore blockage; ACFC10's pores can accommodate acetone despite being obstructed enough to prevent TMB adsorption.

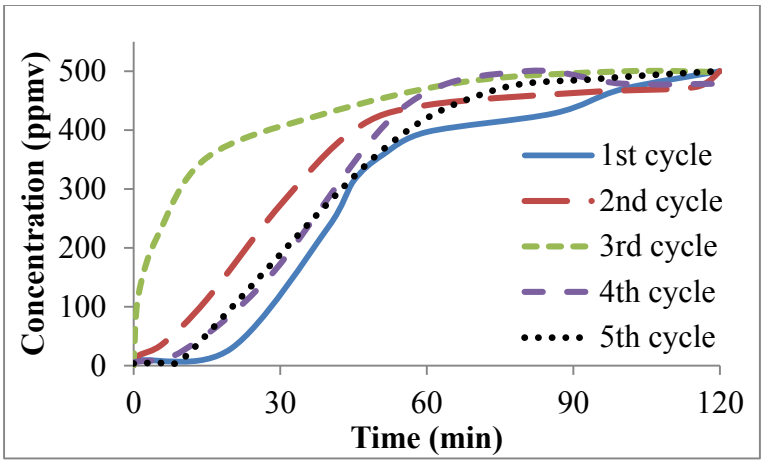

Figure 2-5. Breakthrough curves for adsorption of 1,2,4-trimethylbenzene (1st to 3rd cycles) followed by adsorption of acetone (4th and 5th cycles) on ACFC10 (regenerated at 288 °C)

We propose that observed reductions in adsorption capacity, and increases in heel, are attributed to the formation and deposition of solid carbon species (e.g., coke) on the surface of the ACFCs. Such a mechanism for heel formation is rare and has, to the best of our knowledge, only been suggested in the literature once before for the adsorption of promethazine hydrochloride (PMET) on powdered activated carbon (PAC) and regenerated with microwave heating at 300-500 °C (Caliskan et al. 2012). Thermal reaction/degradation of TMB at high temperatures is the expected cause for carbon accumulation. Carbon species formed and deposited on the ACFC surface during regeneration block adsorption sites, decreasing TMB adsorption during subsequent cycles.

Heel formation is more commonly attributed to strong physical adsorption (Thakkar et al. 1987), oligomerization (Lu et al. 2007), or chemisorption (Lashaki et al. 2012). Physical adsorption is exothermic, causing heel to decrease with increasing temperature (Hubbard 2002). In this work, increasing temperature

caused increased heel, removing the possibility of strong physical adsorption as a heel formation mechanism. Oligomerization has only been documented in the aqueous phase and typically occurs through oxygen functional groups associated with the adsorbate/adsorbent (Vidic et al. 1997) and/or the presence of oxygen in the aqueous system (Lu et al. 2004, Lu et al. 2007), negating its likelihood in the described experiments.

To differentiate between chemisorption and adsorbate decomposition as heel formation mechanisms, regenerated samples were exposed to temperatures > 500 °C using TGA/DTG to identify the strength of adsorbate-adsorbent interaction (Figure 2-6). Coke deposited from degradation of aromatics is expected to be very stable, even at high temperatures (Froment et al. 1994), while chemisorbed species may be removed (Lashaki et al. 2012).

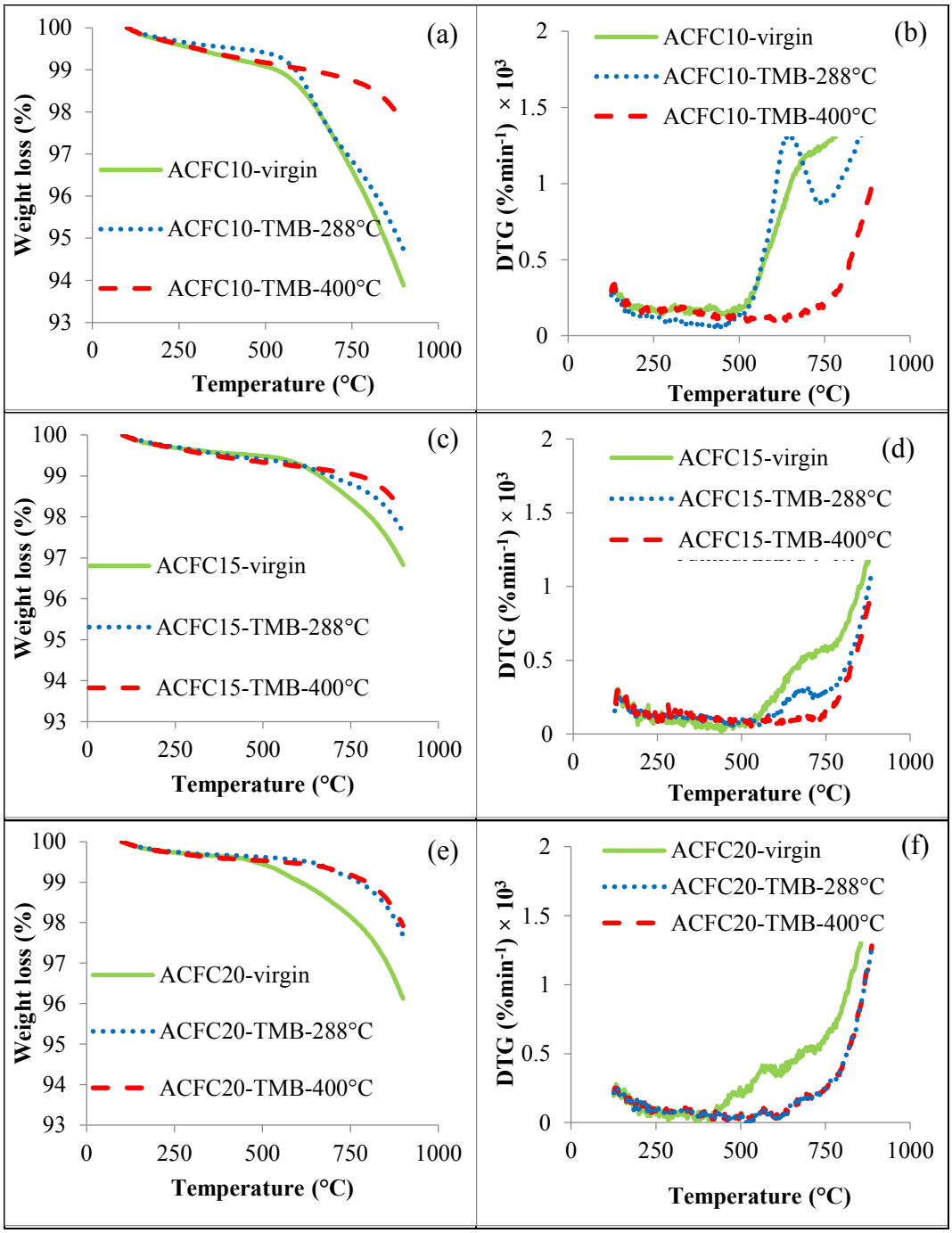

Figure 2-6. Thermogravimetric and differential thermogravimetric analyses (TGA/DTG) of ACFC samples: (a) TGA of ACFC10, (b) DTG of ACFC10, (c) TGA of ACFC15, (d) DTG of ACFC15, (e) TGA of ACFC20, and (f) DTG of ACFC20. The numbers in the legend correspond to regeneration temperature

Weight loss for the used samples, in every case and independent of regeneration temperature, is less than virgin ACFC (Figure 2-6-a, c, and e). Furthermore, weight loss of samples regenerated at 400 °C (those with higher heel) was less than samples regenerated at 288 °C. This indicates that carbon species formed during adsorption/regeneration cycling are strongly attached to the ACFC surface and cannot be removed at temperatures as high as 900 °C. This is inconsistent with results in the literature for strong physical adsorption, oligomerization, or even many cases of chemisorption, where TGA mass losses increase with heel formation (Lashaki et al. 2012). This justifies a unique heel formation mechanism in these experiments.

DTG results provide additional information about the nature of heel accumulated on ACFCs. A DTG peak at approximately 650 °C is evident for ACFC10 and ACFC15 samples regenerated at 288 °C and is not present for samples regenerated at 400 °C. This peak is most intense for ACFC10, followed by ACFC15 and may be associated with desorption of chemisorbed TMB. This indicates that while coking is still expected to occur at 288 °C, chemisorption may also contribute to heel. Since ACFC10 has the narrowest pores, chemisorption may be favored, resulting in a larger DTG peak (Figure 2-6). For samples regenerated at 400 °C, no DTG peaks are evident, indicating that no specific form of heel (including chemisorption that is postulated to occur when regenerating at 288 °C) is removed over the assessed temperature range – the formed heel is much more stable. This is consistent with the coke formation mechanism discussed earlier because generated coke species have high thermal stability (Ania

et al. 2004). Since all tested ACFCs have similar heels for regeneration at 288 °C, gradually smaller DTG peaks at 650 °C for ACFC15 and ACFC20 indicate that carbonization and coke deposition is more prominent for the larger pore volume samples. Similarly, for results at 400 °C, negligible mass losses are recorded for all samples despite variable amounts of heel, with ACFC20 having the highest. This again indicates that coke formation is most notable for ACFC20.

While our results strongly suggest an adsorbate decomposition mechanism as the source of heel, the question that remains is *why* coking occurs under the conditions described in this work and in work by Galiscan et al. (Caliskan et al. 2012), but it has not been otherwise reported for organic vapor desorption from activated carbon adsorbents. In nearly every other VOC-activated carbon desorption study, heel formation decreases with increasing desorption temperature, attributed to a larger difference between VOC boiling point and surrounding temperatures favoring the release of strongly adsorbed (including chemisorbed) species. In this work, however, and the microwave work reported elsewhere (Caliskan et al. 2012), low temperature regeneration causes minimal heel formation, but regeneration at increased temperatures results in coking and increased heel. An endothermic reaction, such as organic compound decomposition (Fahim et al. 2009), that results in carbonization can explain the observations. In our experiments, therefore, increasing regeneration temperature from 288 °C to 400 °C increases carbon deposition on ACFC, causing further decreases in adsorption capacity and increases in heel. It should be noted that the authors of the highlighted microwave desorption study (Caliskan et al. 2012) were

the first to report the possibility of desorbate decomposition resulting in coking. However, they attributed coke deposition to reactions dependent on microwave energy, implying that microwaves are essential for carbonization to occur. Results presented here, for resistive heating, indicate that such an explanation is not unique for microwave desorption.

While the previous work used microwave heating and this work uses resistive heating, the commonality between the two studies is that heating rates are fast. For the microwave work, reported heating rates are ca. 60 – 70 $^{\circ}$C/min (the authors report that 5 – 7 min are required to reach temperatures from 300 – 500 $^{\circ}$C). In our work, the heating rate used to reach the target regeneration temperature is ca. 70 °C/min. These rates are exceedingly rapid compared to other studies available in the literature, where carbon adsorbents are heated at ca. 10 °C/min to achieve the set-point desorption temperature (Wang et al. 2009, Fayaz et al. 2011, Lashaki et al. 2012). This means that, in this work, adsorbate may remain on (or near) the adsorbent once high temperatures are achieved, allowing for carbonization to occur. Whether carbonization occurs when the TMB is adsorbed or shortly after it is desorbed (gas phase), this rapid heating can explain why coking has only been reported in the two described works. This is further justified by comparing cumulative heel on ACFCs when regenerating at 400 °C (Figure 2-4). Since adsorption capacity is highest for ACFC20, followed by ACFC15 and ACFC10, more TMB is available and exposed to the quickly achieved high desorption temperatures, resulting in more carbonization, coke deposition, and heel. If TMB decomposition occurs in the gas phase (as opposed

to the adsorbed phase), ACFC20 can generate increased gas phase concentrations of TMB, also potentially resulting in increased coke formation compared to the other adsorbents. As expected, ACFC15 similarly causes more heel than ACFC10. Note that at 288 °C, when heel associated with coking is less significant for all samples, the difference between cumulative heel of ACFC10, ACFC15, and ACFC20 was small.

The implications of these findings are significant. Microwave and resistive heating are consistently praised in the literature for providing high heating rates that favor rapid desorption times and low energy consumption (Ania et al. 2004, Sullivan et al. 2004a, Sullivan et al. 2004b, Ania et al. 2005, Caliskan et al. 2012). The results reported here, combined with past research on microwave desorption (Ania et al. 2004, Ania et al. 2005, Caliskan et al. 2012), suggest that high heating rates, in select cases, can be a detriment to these methods, causing more heel formation attributed to adsorbate decomposition and carbon deposition on the adsorbent. These results suggest that there is an optimum heating rate for microwave and resistive heating that allows faster desorption with minimum adsorbates decomposition and coke formation.

2-4. References

Ania, C. O., J. A. Menendez, J. B. Parra and J. J. Pis (2004). "Microwave-induced regeneration of activated carbons polluted with phenol. A comparison with conventional thermal regeneration." Carbon **42**(7): 1383-1387.

Ania, C. O., J. B. Parra, J. A. Menendez and J. J. Pis (2005). "Effect of microwave and conventional regeneration on the microporous and mesoporous network and on the adsorptive capacity of activated carbons." Microporous and Mesoporous Materials **85**(1–2): 7-15.

Caliskan, E., J. M. Bermudez, J. B. Parra, J. A. Menendez, M. Mahramanlıoğlu and C. O. Ania (2012). "Low temperature regeneration of activated carbons using microwaves: Revising conventional wisdom." Journal of Environmental Management **102**(0): 134-140.

Carratala-Abril, J., M. A. Lillo-Rodenas, A. Linares-Solano and D. Cazorla-Amorós (2010). "Regeneration of activated carbons saturated with benzene or toluene using an oxygen-containing atmosphere." Chemical Engineering Science **65**(6): 2190-2198.

Chang, P. H. and S. EseI (1998). Effect of carbon surface on thermal decomposition of hydrocarbons. ABSTRACTS OF PAPERS OF THE AMERICAN CHEMICAL SOCIETY, AMER CHEMICAL SOC 1155 16TH ST, NW, WASHINGTON, DC 20036 USA.

Dabrowski, A., P. Podkoscielny, Z. Hubicki and M. Barczak (2005). "Adsorption of phenolic compounds by activated carbon: a critical review." Chemosphere **58**(8): 1049-1070.

Dombrowski, K., C. Lehmann, P. Sullivan, D. Ramirez, M. Rood and K. Hay (2004). "Organic vapor recovery and energy efficiency during electric regeneration of an activated carbon fiber cloth adsorber." Journal of Environmental Engineering **130**(3): 268-275.

Fahim, M. A., T. A. Al-Sahhaf and A. Elkilani (2009). Fundamentals of Petroleum Refining, Elsevier Science.

Fayaz, M., H. Wang, M. Lashaki, Z. Hashisho, J. H. Philips and J. E. Anderson (2011). Accumulation of Adsorbed of Organic Vapors from Automobile Painting Operations on Bead Activated Carbon. Air and Waste Management Association Annual Meeting Conference and Exhibition, Orlando.

Ferro-Garcia, M. A., J. P. Joly, J. Rivera-Utrilla and C. Moreno-Castilla (1995). "Thermal desorption of chlorophenols from activated carbons with different porosity." Langmuir **11**(7): 2648-2651.

Froment, G. F. and B. Delmon (1994). Catalyst Deactivation, Elsevier Science.

Golovoy, A. and J. Braslaw (1981). "Adsorption of automotive paint solvents on activated carbon: I. Equilibrium adsorption of single vapors." Journal of the Air Pollution Control Association **31**(8): 861-865.

Grant, T. M. and C. J. King (1990). "Mechanism of irreversible adsorption of phenolic compounds by activated carbons." Industrial & Engineering Chemistry Research **29**(2): 264-271.

Ha, S. R. and S. Vinitnantharat (2000). "Competitive removal of phenol and 2,4-dichlorophenol in biological activated carbon system." Environmental Technology **21**(4): 387-396.

Hashisho, Z., H. Emamipour, M. J. Rood, K. J. Hay, B. J. Kim and D. Thurston (2008). "Concomitant adsorption and desorption of organic vapor in dry

and humid air streams using microwave and direct electrothermal swing adsorption." Environmental Science Technolology **42**(24): 9317-9322.

Hashisho, Z., M. J. Rood, S. Barot and J. Bernhard (2009). "Role of functional groups on the microwave attenuation and electric resistivity of activated carbon fiber cloth." Carbon **47**(7): 1814-1823.

Hubbard, A. T. (2002). Encyclopedia of Surface and Colloid Science, Taylor & Francis.

Jahandar Lashaki, M., M. Fayaz, S. Niknaddaf and Z. Hashisho (2012). "Effect of the adsorbate kinetic diameter on the accuracy of the Dubinin–Radushkevich equation for modeling adsorption of organic vapors on activated carbon." Journal of Hazardous Materials **241–242**(0): 154-163.

Kennes, C. and M. C. Veiga (2013). Air Pollution Prevention and Control: Bioreactors and Bioenergy, Wiley.

Kim, B. R. (2011). "VOC emissions from automotive painting and their control: A review." Environmental Engineering Research **16**(1): 1-9.

Klinowski, J. and P. J. Barrie (1989). Recent Advances in Zeolite Science, Elsevier Science.

Lashaki, M., M. Fayaz, H. Wang, Z. Hashisho, J. H. Philips, J. E. Anderson and M. Nichols (2012). "Effect of adsorption and regeneration temperature on irreversible adsorption of organic vapors on beaded activated carbon." Environmental Science & Technology **46**(7): 4083-4090.

Lo, S. Y. (2000). Characterization of the chemical, physical, thermal and electrical properties of a series of activated carbon fiber cloths, University of Illinois at Urbana–Champaign. **MSc**.

Lordgooei, M., K. R. Carmichael, T. W. Kelly, M. J. Rood and S. M. Larson (1996). "Activated carbon cloth adsorption-cryogenic system to recover toxic volatile organic compounds." Gas Separation & Purification **10**(2): 123-130.

Lowell, S. and J. E. Shields (1991). Powder Surface Area and Porosity, Springer.

Lu, Q. and G. A. Sorial (2004). "Adsorption of phenolics on activated carbon–impact of pore size and molecular oxygen." Chemosphere **55**(5): 671-679.

Lu, Q. and G. A. Sorial (2007). "The effect of functional groups on oligomerization of phenolics on activated carbon." Journal of Hazardous Materials **148**(1–2): 436-445.

Mallouk, K. E., D. L. Johnsen and M. J. Rood (2010). "Capture and recovery of isobutane by electrothermal swing adsorption with post-desorption liquefaction." Environmental Science & Technology **44**(18): 7070-7075.

Mangun, C. L., R. D. Braatz, J. Economy and A. J. Hall (1999). "Fixed Bed Adsorption of Acetone and Ammonia onto Oxidized Activated Carbon Fibers." Industrial & Engineering Chemistry Research **38**(9): 3499-3504.

Ramos, M. E., P. R. Bonelli, A. L. Cukierman, M. M. L. Ribeiro Carrott and P. J. M. Carrott (2010). "Adsorption of volatile organic compounds onto activated carbon cloths derived from a novel regenerated cellulosic precursor." Journal of Hazardous Materials **177**(1–3): 175-182.

Sidheswaran, M. (2012). "Energy Efficient Indoor VOC Air Cleaning with Activated Carbon Fiber (ACF) Filters."

Subrenat, A., J. N. Baléo, P. Le Cloirec and P. E. Blanc (2001). "Electrical behaviour of activated carbon cloth heated by the joule effect: desorption application." Carbon **39**(5): 707-716.

Sullivan, P., M. Rood, K. Dombrowski and K. Hay (2004). "Capture of organic vapors using adsorption and electrothermal regeneration." Journal of Environmental Engineering **130**(3): 258-267.

Sullivan, P. D., M. J. Rood, G. Grevillot, J. D. Wander and K. J. Hay (2004). "Activated carbon fiber cloth electrothermal swing adsorption system." Environmental Science & Technology **38**(18): 4865-4877.

Sullivan, P. D., B. R. Stone, Z. Hashisho and M. Rood (2007). "Water adsorption with hysteresis effect onto microporous activated carbon fabrics." Adsorption **13**(3-4): 173-189.

Thakkar, S. and M. Manes (1987). "Adsorptive displacement analysis of many-component priority pollutants on activated carbon." Environmental Science Technology **21**(6): 546-549.

Vidic, R. D., C. H. Tessmer and L. J. Uranowski (1997). "Impact of surface properties of activated carbons on oxidative coupling of phenolic compounds." Carbon **35**(9): 1349-1359.

Vinitnantharat, S., A. Baral, Y. Ishibashi and S. R. Ha (2001). "Quantitative bioregeneration of granular activated carbon loaded with phenol and 2,4-dichlorophenol." Environmental Technology **22**(3): 339-344.

Wang, Q., X.-y. Liang, R. Zhang, C.-j. Liu, X.-j. Liu, W.-m. Qiao, L. Zhan and L.-c. Ling (2009). "Preparation of polystyrene-based activated carbon spheres and their adsorption of dibenzothiophene." New Carbon Materials **24**(1): 55-60.

CHAPTER 3 INFLUENCE OF DESORPTION PURGE FLOW AND HEATING RATES ON HEEL BUILDUP ON ACTIVATED CARBON FIBER CLOTH

A version of this chapter will be submitted for publication. Reproduced with permission from Saeid Niknaddaf, John D. Atkinson, Abedeh Gholidoust, Mohammadreza Fayaz, Zaher Hashisho, John H. Philips, James E. Anderson, Mark Nichols

3-1. Introduction

Adsorption is widely used method for controlling volatile organic compounds (VOCs), which have potential impacts on humans and the environment (Ramos et al. 2010, Lashaki et al. 2012). Adsorption is low cost, provides the opportunity for adsorbate recovery and adsorbent reuse, and has high efficiency for low concentrations of VOCs (Dabrowski et al. 2005, Mallouk et al. 2010, Sidheswaran 2012). Accumulation of mass inside adsorbent pores, or heel buildup, is a common challenge associated with adsorption (Lashaki et al. 2012). Activated carbon fiber cloth (ACFC) is used for VOC adsorption because it is ash free and provides high surface area, micropore volume, and adsorption capacity (Hashisho et al. 2009, Ramos et al. 2010). Because it consists of continuous fibers, ACFC is more electrically conductive than many other activated carbons, making it a useful material for electrical swing adsorption (ESA), where heat provided by resistive heating causes VOC desorption (Subrenat et al. 2001, Dombrowski et al. 2004, Mallouk et al. 2010). ESA provides high regeneration efficiency, low energy consumption, and low carrier gas use compared to other heating methods (Sullivan et al. 2004a, Sullivan et al. 2004b, Mallouk et al. 2010). Also, unlike steam regeneration, ESA does not require separation of condensed desorbate from water nor drying after regeneration (Sullivan et al. 2004b).

Strong physical adsorption (Thakkar et al. 1987), chemical adsorption (Lowell et al. 1991, Ha et al. 2000, Lashaki et al. 2012), oligomerization (Vinitnantharat et al. 2001, Lu et al. 2004b, Lu et al. 2004a), and desorbate

decomposition (Ania et al. 2004, Ania et al. 2005, Caliskan et al. 2012) are heel buildup mechanisms that have been investigated extensively in adsorption from aqueous phase (Grant et al. 1990, Ferro-Garcia et al. 1995, Lu et al. 2007, Caliskan et al. 2012), and in less detail in the gas phase (Fayaz et al. 2011, Lashaki et al. 2012). While other heel buildup mechanisms are associated with adsorption parameters, proclivity for desorbate decomposition depends strongly on regeneration conditions. After adsorption of phenol and salicylic acid from aqueous solution, Ania *et al.* showed that phenol and salicylic acid decompose at temperatures achieved during microwave and conventional heating regeneration at 850 °C, blocking adsorbent pores and reducing its capacity. They suggested that adsorbate remaining inside pores during regeneration turns to coke because of exposure to high temperatures (Ania et al. 2004, Ania et al. 2005). Caliskan *et al.* observed similar decomposition during adsorption/regeneration cycles with promethazine hydrochloride (PMET) on activated carbon. They found that for regeneration at 500 °C, adsorption capacity loss during cycling is 60% higher when regenerating with microwave energy compared to conductive heating. The authors suggest that PMET decomposition is accelerated in the presence of microwaves because the polar adsorbate readily absorbs microwave irradiation (Caliskan et al. 2012). We previously adsorbed TMB (a bulky molecule with relatively low diffusion rate) on ACFC and found that more desorbate decomposition was incurred when regenerating with high heating rates (70 °C/min), at 400 °C compared to 288°C, resulting in decreased pore volume, surface area, adsorption capacity, and regeneration efficiency. However, the effect

of heating rate on regeneration efficiency during adsorption/regeneration cycles has not been clearly described. Ferro-Garcia *et al.* showed that for activated carbon saturated with chlorophenol in aqueous solution, high heating rates favored transformation of physisorbed chlorophenols to chemisorbed species, or solid residues during regeneration (Ferro-Garcia et al. 1995). Roman *et al.* similarly conducted variable heating rate experiments on activated carbon saturated with nitrophenol in aqueous solution, showing that lower heating rates slightly improve regeneration efficiency (Roman et al. 2013). They attributed these effects to longer regeneration times resulting in further desorption for samples regenerated at lower heating rates (Roman et al. 2013). Although previous studies confirmed that desorbate decomposition or transformation of desorbate might happen during faster regeneration of organic compound and this phenomena can alter regeneration performance of adsorbent, they didn't acknowledge the effect of heating rate as a major parameter in regeneration performance and there is no clear study, to the best of our knowledge that explains the effect of heating rate on heel buildup and adsorption capacity during consecutive cycles of the gas phase adsorption.

Regeneration purge gas flow rate should also be investigated to identify its impact on regeneration efficiency and heel buildup. An *et al* reported that flow rate has a little effect on outlet concentration during CO_2 desorption, but emphasized that a low flow rate is preferred because less heat is lost due to convection (An et al. 2010). On the other hand, Subrenat and Le Cloirec found that increasing the purge gas flow rate during regeneration decreased the local

concentration (close to the external surface of the ACFC) in gas phase by dilution. This improved the desorption kinetics and increased the total amount desorbed for a fixed duration (Subrenat et al. 2004). Since local concentration during regeneration and desorption kinetics might affect organic compound decomposition and flow rate influences desorption kinetics and desorbate concentration, regeneration flow rate is expected to change regeneration efficiency or heel buildup, However there is no detailed information, to the best of our knowledge, about the effect of regeneration flow rate on heel buildup during adsorption of volatile organic compounds. Understanding conditions that promote desorbate decomposition will improve efficiency and adsorbent lifetime during adsorption/regeneration cycling. This will help to design new VOC adsorption systems or optimize the existing systems to achieve better performance of adsorbent during adsorption/regeneration cycling. The objective of this work, therefore, is to identify and report the effect of regeneration heating and flow rate on heel buildup during adsorption/regeneration cycling with a volatile organic compound that shows strong diffusion resistance.

3-2. Materials and Methods

3-2-1. Adsorbent and Adsorbate

Activated carbon fiber cloth (ACC-5092-15, or ACFC15) prepared from phenol-formaldehyde resin (Nippon Kynol Company) was the adsorbent and 1,2,4-trimethylbenzene (TMB – 98%, Acros Organics) was the adsorbate for all results presented herein. Virgin ACFC was heated for 2 hours at 400 °C prior to

use to remove adsorbed impurities such as water vapor and residual organic compounds.

3-2-2. Experimental Set-Up and Methods

The experimental setup includes an adsorption/regeneration tube containing an ACFC cartridge, an adsorbate generation system, a gas detection system, a heat application module, and a data acquisition and control system (DAC) (Figure 3-1). The adsorption/regeneration tube consists of a quartz tube with 7.3 cm inner diameter and 40 cm length. The ACFC cartridge consists of 3.5 g ACFC (22 cm length, 10 cm width) wrapped around two stainless steel electrode tubes (1.65 cm outer diameter), making a 3-layer annular cartridge. The top electrode tube was used for introducing the adsorption stream into the cartridge while the bottom one was sealed to force the gas to go through the cartridge.

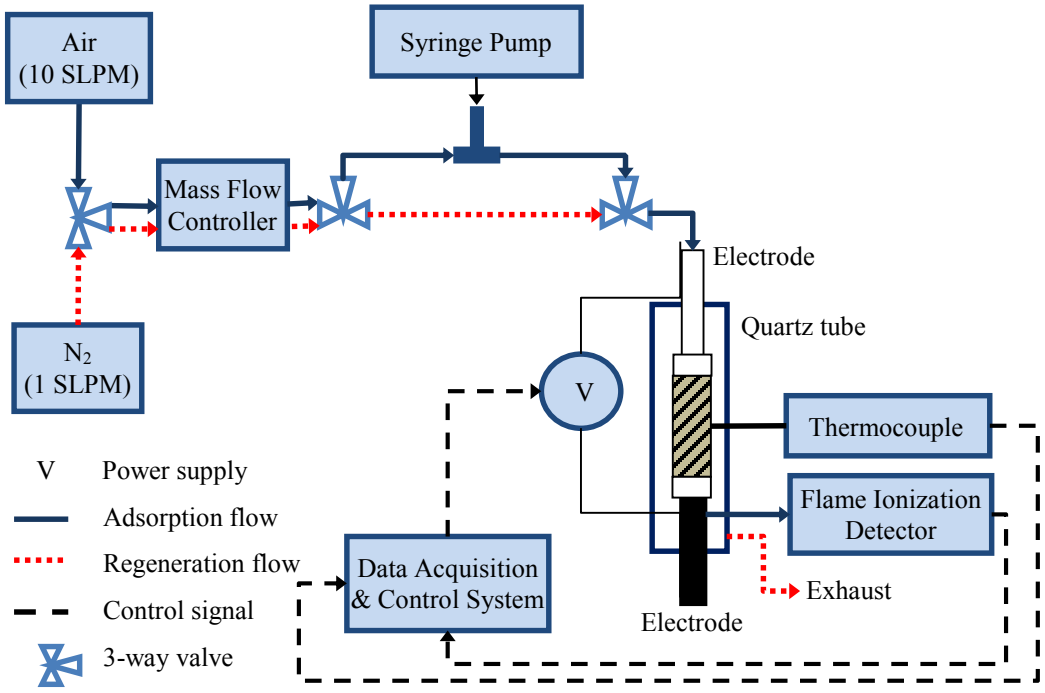

Figure 3-1. Schematic diagram of the adsorption/regeneration set-up

500 ppm_v of adsorbate was used for all experiments. The adsorbate generation system includes a syringe pump (New Era Inc., NE-300) to inject liquid TMB into a 10 SLPM (standard conditions are 20 °C and 1 atm) dry air stream. Organic vapor concentration at the Adsorption tube's outlet was continuously (2 min sampling frequency) measured during adsorption using a flame ionization detector (FID, Baseline-Mocon Inc., series 9000). The FID was calibrated before each adsorption test with the generated organic vapor stream using a bypass line.

For heat application, a silicon-controlled rectifier (SCR) applied voltage to both sides of the ACFC cartridge. ACFC temperature during adsorption and regeneration was measured using a 1.6 mm outer diameter, ungrounded, type K thermocouple (Omega). The DAC system includes a data logger (National

instruments, Compact DAQ) equipped with analog input/output modules and a LabVIEW program to monitor and record the adsorption tube's outlet VOC concentration and temperature. To obtain the set point temperature during regeneration, a proportional-integral-derivative control algorithm was used. Before starting the heating, 1 SLPM of N_2 was used for 5 min to purge the oxygen out of the quartz tube. 1 SLPM of N_2 and 70 °C/min heating rate were the baseline regeneration conditions. Different regeneration flow rates (0.1, 0.5, 1, 2, 5 SLPM) and heating rates (5, 10, 20, 40, 70, 100 °C/min) were investigated. Independent of conditions, regeneration was completed at constant temperature (400 °C) for 100 min followed by cooling (i.e., no heat application) for 30 min while purging continuously with nitrogen.

After FID calibration, the VOC laden air stream was introduced to the adsorption tube and measurement of the outlet concentration began, generating a breakthrough curve. For all tests, adsorption was completed at 25 °C and continued for 2 h, ensuring TMB breakthrough and ACFC saturation. Adsorption capacity was calculated after each cycle as follows:

$$Amount\ adsorbed\ or\ adsorption\ capacity\ (\text{wt}\%) = \frac{\text{Cartridge weight after adsorption} - \text{Cartridge weight before adsorption}}{\text{Weight of virgin ACFC}} \text{X100}$$

Reduction in ACFC adsorption capacity from the 1st cycle to the 5th cycle was calculated as follows:

$$Capacity\ loss(\%) = \frac{\text{Amount adsorbed after } 1^{st} \text{ cycle} - \text{Amount adsorbed after } 5^{th} \text{ cycle}}{\text{Amount adsorbed after } 1^{st} \text{ cycle}} \times 100$$

After regeneration, the ACFC cartridge was cooled to 25 °C and weighed. The difference between weights before adsorption and after regeneration is the amount of heel buildup during that cycle. The total heel buildup after five adsorption/regeneration cycles:

$$Heel\ buildup\ (\text{wt}\%) = \frac{\text{Weight after } 5^{th} \text{ regeneration cycle} - \text{Weight before } 1^{st} \text{ adsorption cycle}}{\text{Weight of virgin ACFC}} \text{X}100$$

3-3. Results & Discussion

TMB breakthrough curves for different heating rates are presented in Figure 3-2. Increasing heating rate from 5 °C/min to 100 °C/min decreased ACFC performance during continued use, as evidenced by earlier breakthrough times ($t_{1\%}$, when the outlet concentration equals 1% of the inlet concentration) associated with subsequent cycles (Table 3-1). When heating at 5 °C/min, there is < 25% change in breakthrough time between the first and last cycles. Increasing the heating rate from 5 to 100 °C/min decreased breakthrough times for consecutive cycles. For 100 °C/min, breakthrough time decreased by 64% for the second cycle, and immediate breakthrough occurred after the third cycle.

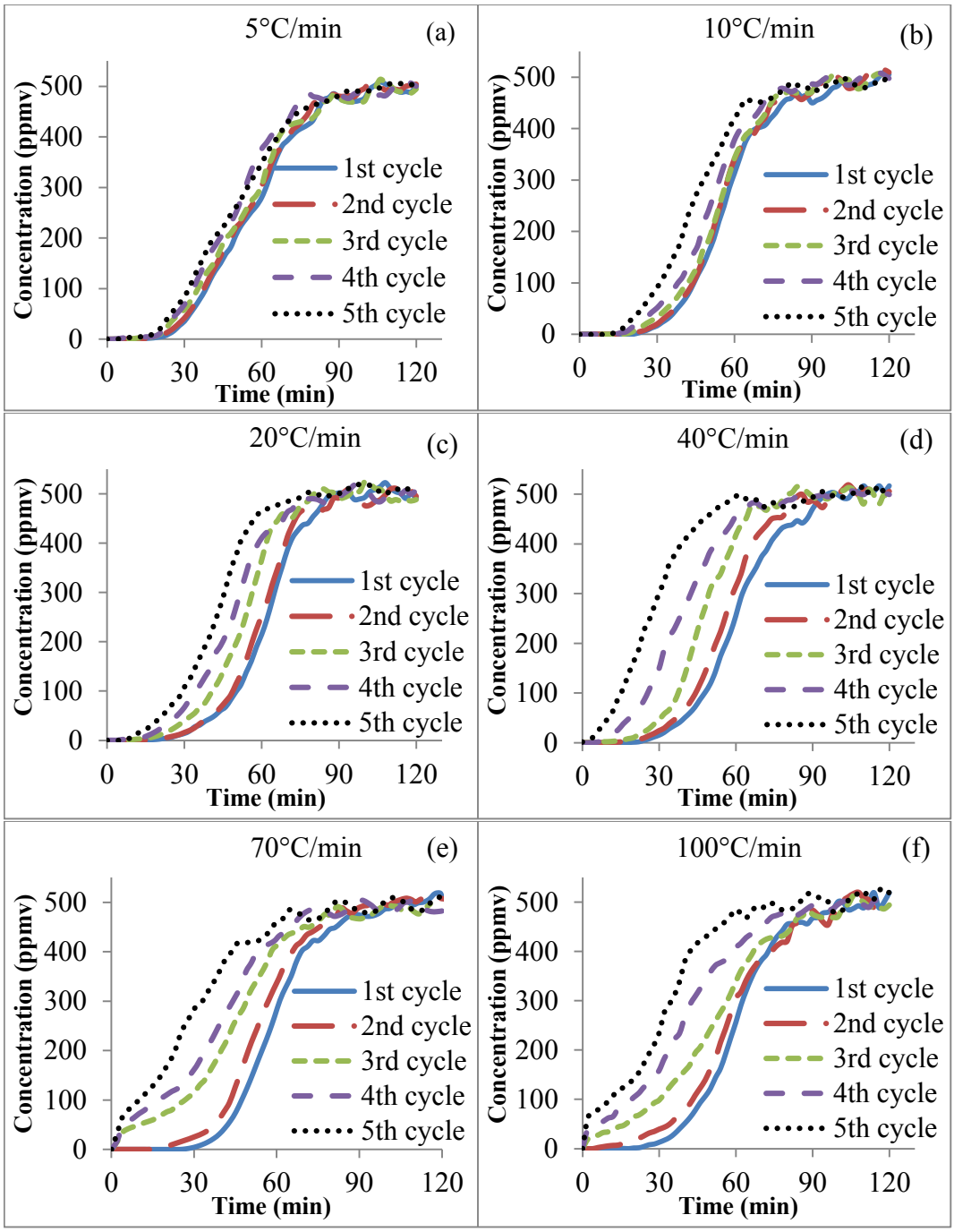
5°C/min
(a)
Concentration (ppmv)
500
400
300
200
100
0
0
30
60
90
120
Time (min)
1st cycle
2nd cycle
3rd cycle
4th cycle
5th cycle
10°C/min
(b)
20°C/min
(c)
40°C/min
(d)
70°C/min
(e)
100°C/min
(f)

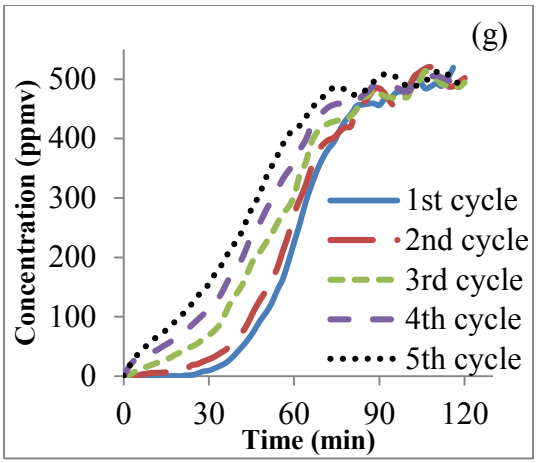

Figure 3-2. Adsorption breakthrough curves for 1,2,4-trimethylbenzene on ACFC regenerated at different heating rates: (a) 5 °C/min, (b) 10 °C/min, (c) 20 °C/min, (d) 40 °C/min, (e) 70 °C/min, (f) 100 °C/min, (g) 100 °C/min with 172 min of heating at constant temperature. Regeneration temperature and flow rate were 400 °C and 1 SLPM, respectively.

Table 3-1. Desorption time and reduction in breakthrough time for adsorption of TMB on ACFC at different regeneration conditions

	Ramp Time (min)	**Time at 400 °C (min)**	**Reduction in breakthrough time (%)**			
			Second Cycle	Third Cycle	Forth Cycle	Fifth Cycle
5 °C/min	76	100	6	12	19	23
10 °C/min	38	100	8	14	25	48
20 °C/min	19	100	12	33	45	58
40 °C/min	9.5	100	16	36	68	IBT*
70 °C/min	5.4	100	44	IBT	IBT	IBT
100 °C/min	3.8	100	64	IBT	IBT	IBT
100 °C/min	3.8	172	65	IBT	IBT	IBT
0.1 SLPM	3.8	100	IBT	IBT	IBT	IBT
0.5 SLPM	3.8	100	17	IBT	IBT	IBT
1 SLPM	3.8	100	44	IBT	IBT	IBT
2 SLPM	3.8	100	5	5	10	15
5 SLPM	3.8	100	0	0	6	6
***IBT: Immediate Breakthrough**						

Temperature profile of ACFC cartridge at different heating rates during the first regeneration cycle for all heating rates experiments is presented in Figure 3-3. Since the ACFC temperature is controlled through the DAC and Labview program, using the same control parameters, temperature profiles for the

remaining four cycles (not shown) were the same as that of the first cycle for each heating rate experiment. For all but one (100°C/min-172 min) heating rate experiments, regeneration was completed for 100 min at a steady temperature of 400 °C, although the temperature ramp time was different for different heating rates (Table 3-1).

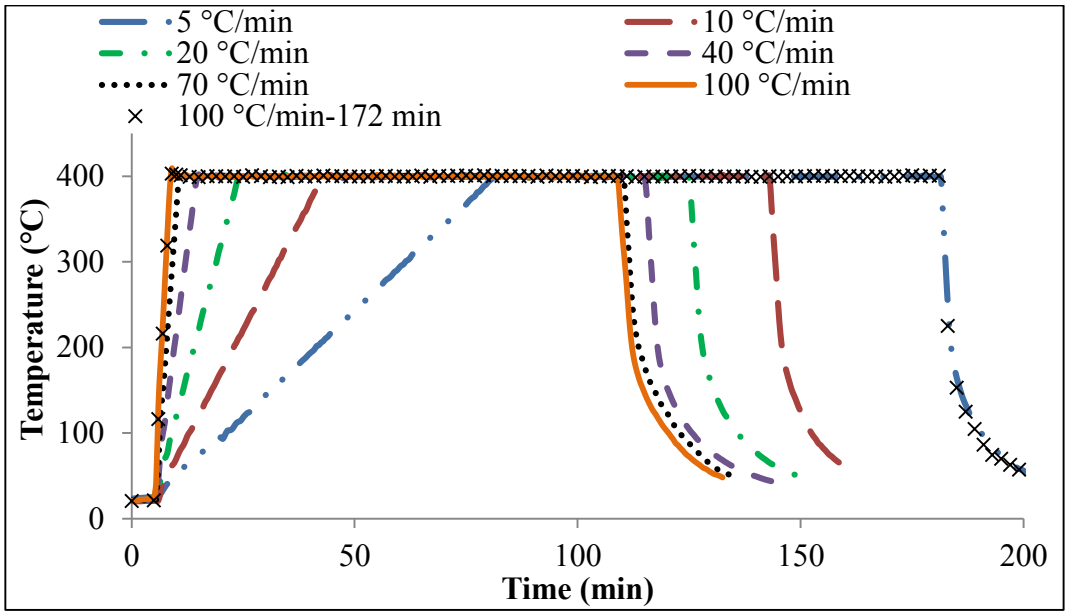

Figure 3-3. Temperature of ACFC cartridge during first regeneration cycle at different heating rates

Increasing the heating rate from 5 °C/min to 100 °C/min increased heel buildup and capacity loss over 5 adsorption/desorption cycles (Figure 3-4). Capacity loss after 5 adsorption/desorption cycles was 8% when regenerating at 5 °C/min and increased to 52% when heating at 100 °C/min. 5-cycle cumulative heel buildup was 4.6%, 6.7%, 8.7%, 9.7%, 10.4%, and 10.5% for samples regenerated with increasing heating rates, respectively. To make sure that the higher heel buildup and capacity loss of 100 °C/min wasn't related to its shorter desorption time, an experiment was completed at 100 °C/min with the same

duration as the lowest heating rate experiments (total desorption time of 176 min for 5 °C/min) (Table 3-1). Heel buildup and capacity loss for this experiment were 10.3% and 51%, respectively, that was similar to the normal experiment at 100 °C/min (Figure 3-4). Breakthrough curve data also confirmed similar behaviour of these two experiments (Figure 3-2-g).

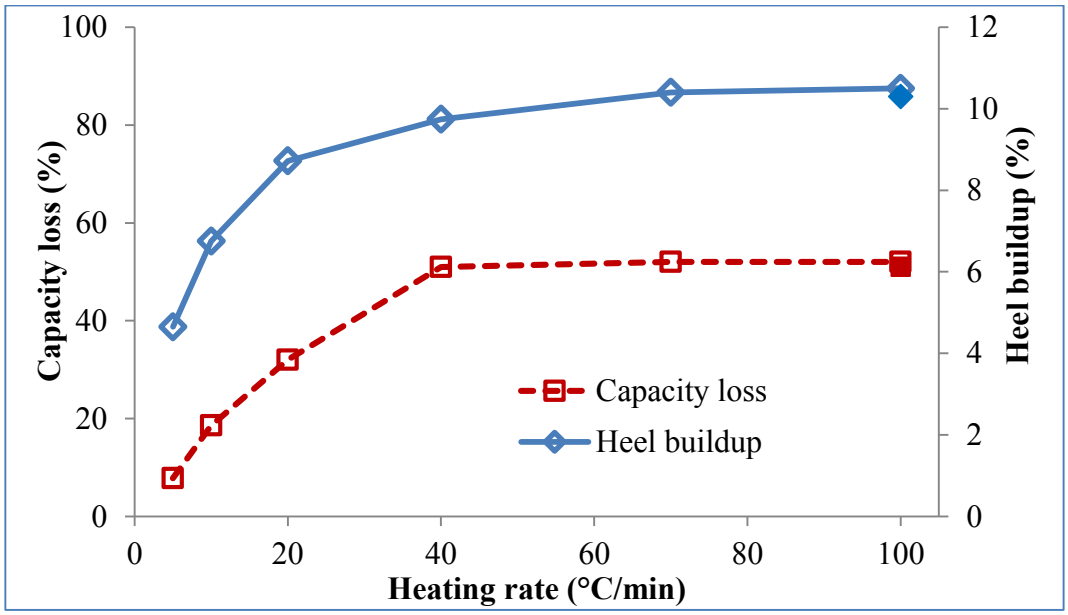

Figure 3-4. Effect of regeneration heating rate on heel buildup and capacity loss of ACFC after five consecutive cycles of TMB adsorption with electrothermal regeneration. Regeneration temperature and N2 flow rate were 400 °C and 1 SLPM, respectively. Solid diamond and square correspond to heel buildup and capacity loss for the experiment at 100 °C/min and 172 min at 400 °C, respectively.

Increasing heel buildup with increasing heating rate is attributed to higher concentrations of desorbate being exposed to high temperatures during regeneration. To confirm this, concentration profile during first regeneration cycle for different heating rates was obtained (Figure 3-5) that is consistent with other authors' observations (Lordgooei et al. 1996, Subrenat et al. 2001, Yu et al. 2007).

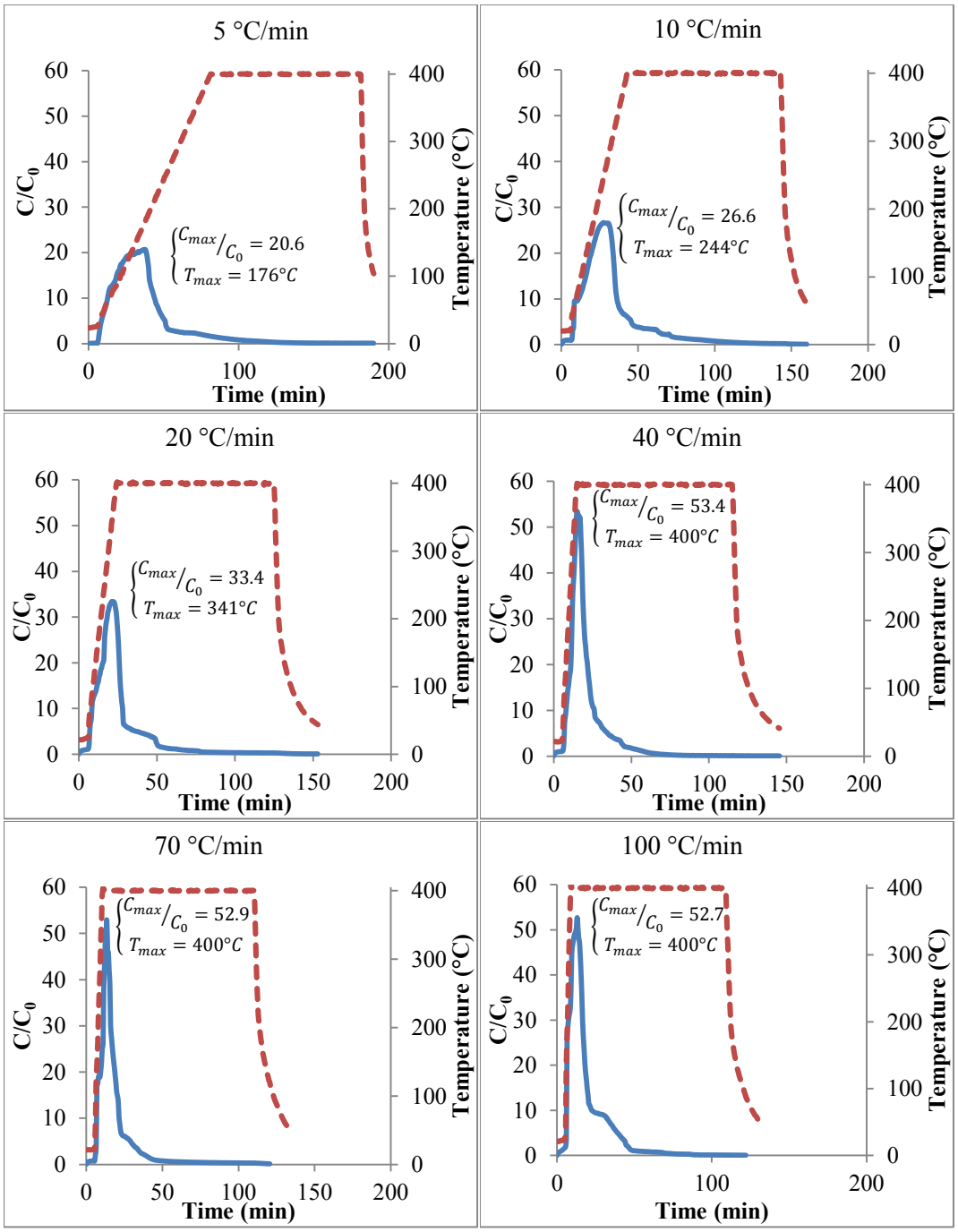

Figure 3-5. Concentration and temperature profile during regeneration of ACFC using different heating rates. Solid lines and Dash lines correspond to concentration and temperature, respectively. C_0 in the primary y-axis is the inlet concentration during adsorption and is equal to 500 ppm.

Outlet concentration increased with increasing temperature to a maximum concentration (C_{max}) reached at a specific temperature (T_{max}), then the concentration decreased rapidly. Increasing heating rate from 5 to 20 °C/min increased both C_{max} and T_{max} (Figure 3-6) which indicates that higher concentration of desorbate is exposed to a higher temperature at higher heating rate. C_{max}/C_0 and T_{max} for heating rates of 5, 10, and 20 °C/min were 20.6 and 176°C, 25.5 and 244°C, and 33.1 and 341°C, respectively. Increasing desorbate concentration and temperature enhances the coking reaction which increases heel buildup and capacity loss (Figure 3-4). After this stage, increasing heating rate from 40 °C/min to 100 °C/min didn't change C_{max} and T_{max}, as the C_{max} was similar (~52-53) and T_{max} was the same (400 °C) for all of these conditions (Figure 3-6). That is the reason why by increasing heating rate more than 40 °C/min, heel buildup and capacity loss didn't change significantly. However, the time interval from the moment temperature reached 400 °C to the moment C_{max} occurred was different for different heating rates. This time interval was 0.5, 2, and 4 min for heating rates of 40, 70, and 100 °C/min, respectively. This indicates that at higher temperature, high concentration of desorbate exposed to high temperature for a longer duration that caused 100 °C/min to have a slightly higher heel buildup compared to 40 and 70 °C/min. In other words, higher heating doesn't always guarantee that the desorbate evolves from the activated carbon faster due to diffusion resistance associated with the bulky molecules being trapped in the carbon's pores (mostly micropores) (Ania et al. 2005, Han et al. 2014) and because this high desorbate concentration exposed sooner to high

temperature during fast heating, more desorbate become coke during regeneration. Mass transfer resistance plays an important role in limiting desorbate transport from inside carbon's pores to the bulk of desorption purge gas and can change the amount of coke deposition and heel buildup. Higher mass transfer increases the desorption rate and causes more desorbate to be removed from the carbon before temperature reaches to higher values. Larger mesopore volume and/or wider micropores can reduce diffusion resistance and increase desorption rates (Carratala-Abril et al. 2010).

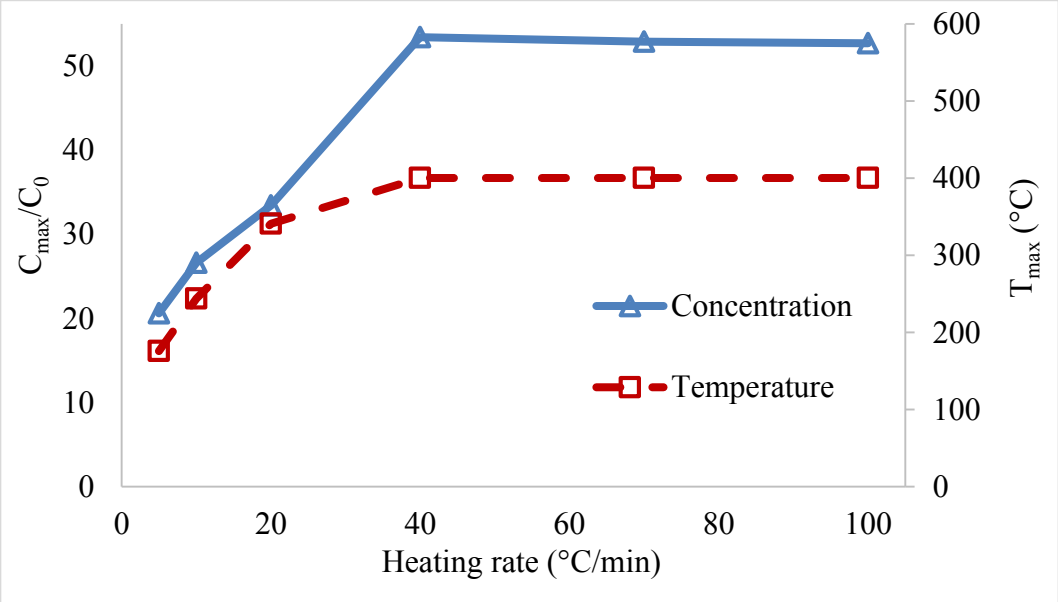

Figure 3-6. Effect of heating rate on maximum concentration (C_{max}) and its corresponding temperature (T_{max}) during desorption of TMB using resistive heating. C_0 in the primary y-axis is the inlet concentration during adsorption and is equal to 500 ppm.

Figure 3-7 shows TMB breakthrough curves for regeneration at 400 °C with different desorption purge gas flow rates. Adsorption/regeneration performance improved with increasing flow rate during regeneration, as reflected

in the breakthrough time (Table 3-1). ACFC's breakthrough time for the sample regenerated with 0.1 SLPM of purge gas decreased dramatically after the first cycle and breakthrough occurred immediately ($t_{1\%}$ = 0 min) after the second cycle (Figure 3-7a). With incremental increases in purge gas flow rates, incremental increases in breakthrough time are noted. At 5 SLPM, breakthrough decreased by only 6% after 5 adsorption/regeneration cycles (Figure 3-7e).

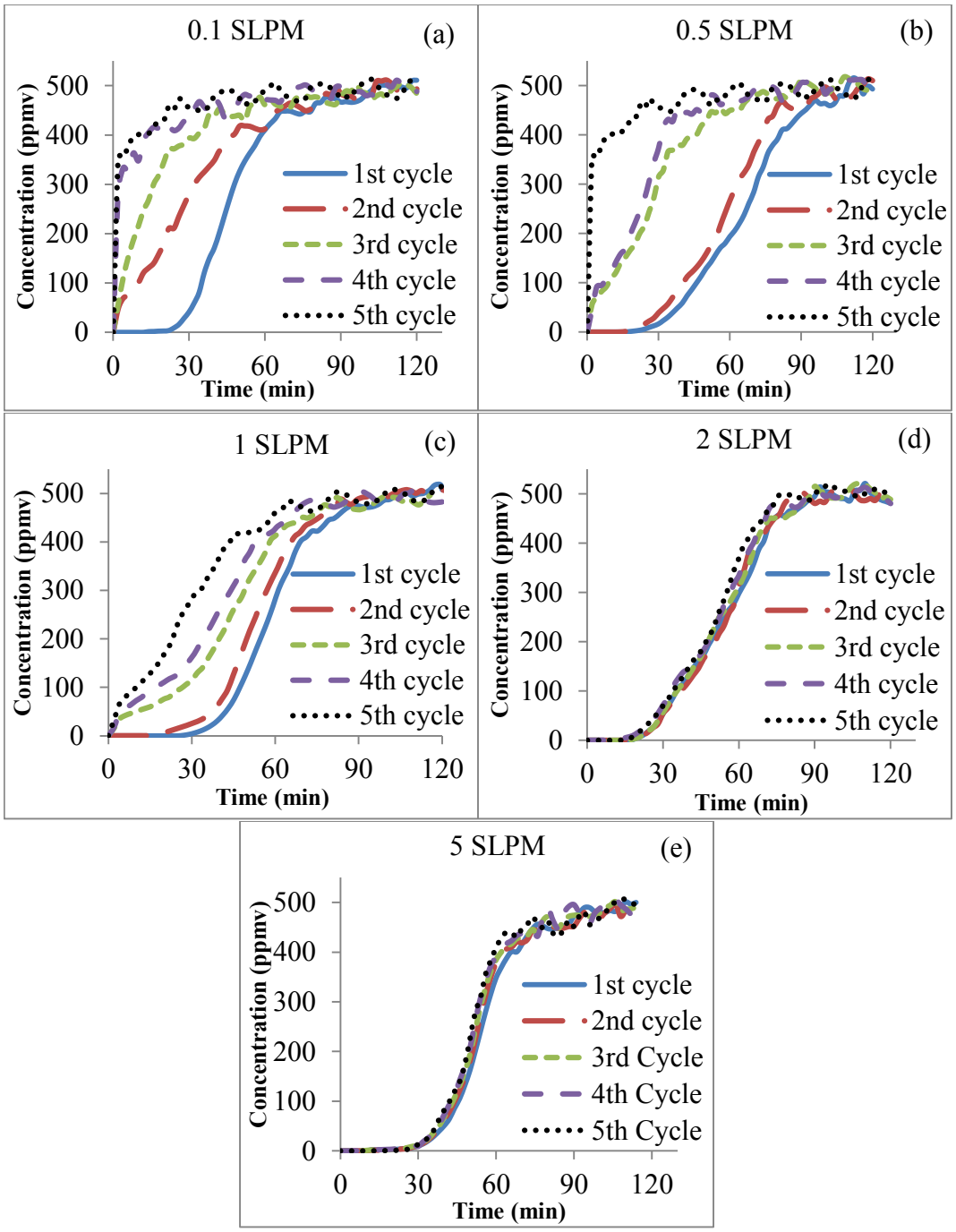

Figure 3-7. Adsorption breakthrough curves for 1,2,4-trimethylbenzene on ACFC using different purge gas flow rate: (a) 0.1 SLPM, (b) 0.5 SLPM, (c) 1 SLPM, (d) 2 SLPM, and (e) 5 SLPM. Regeneration temperature and heating rate were 400 °C and 70 °C/min, respectively.

Figure 3-8 shows the effect of regeneration flow rate on ACFC's heel buildup and capacity loss after 5 adsorption/regeneration cycles. Capacity loss

from the 1st cycle to the 5th cycle was 82% for regeneration at 0.1 SLPM and only 2% for regeneration at 5 SLPM. However, a sharp change in capacity loss occurred for samples regenerated at flow rates < 2 SLPM and, after this point, purge gas flow rate had less influence. Cumulative heel buildup achieved after 5 adsorption/regeneration cycles at different flow rates followed a similar trend as capacity loss. Heel buildup was 14.6%, 11.5%, 10.4%, 2.9%, and 1.4% for the samples regenerated at 0.1, 0.5, 1, 2, and 5 SLPM, respectively. Similar to change in adsorption capacity, major change in heel buildup occurred for flow rates lower than 2 SLPM. Increasing the flow rate from 0.1 SLPM to 2 SLPM decreased heel buildup from 14.6% to 2.9% (6.2 % reduction in heel per 1 SLPM increase of flow rate), while increasing flow rate from 2 SLPM to 5 SLPM reduced the heel build up only from 2.9% to 1.4% (0.5 % reduction in heel per 1 SLPM increase of flow rate). This value is quite important because after 2 SLPM, increasing flow rate will not result in large decrease in heel buildup and capacity loss.

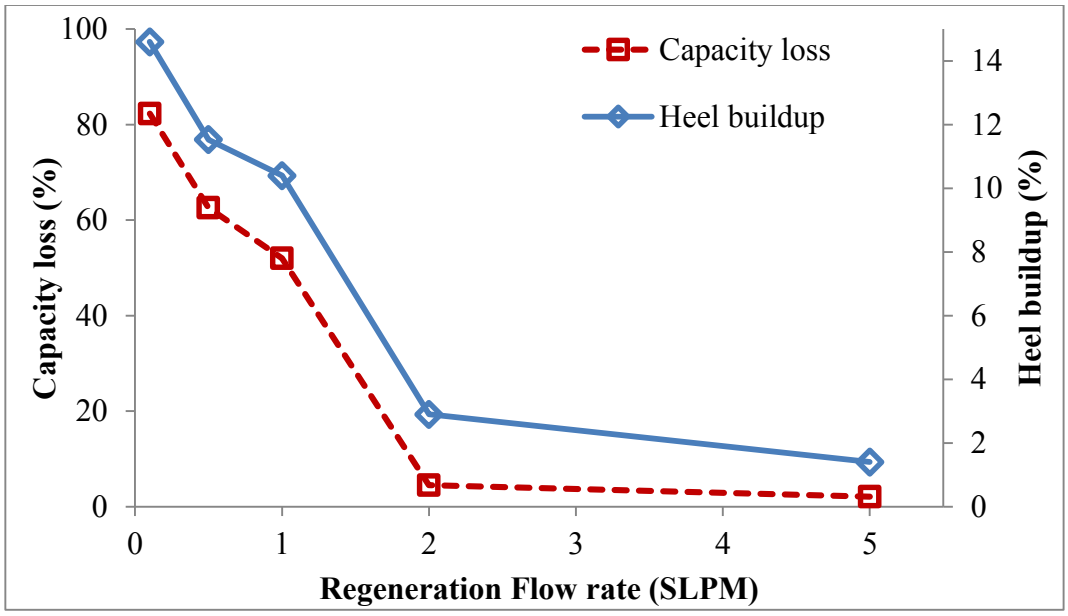

Figure 3-8. Effect of regeneration flow rate on heel buildup and capacity loss of ACFC after five consecutive cycles of TMB adsorption with electrothermal regeneration. Regeneration temperature and heating rate were 400 °C and 70 °C/min, respectively.

Desorption concentration profile for different flow rates (Figure 3-9) confirmed that increasing flow rate decreased the desorbate concentration throughout the regeneration process. As an indication of desorption concentration, C_{max}/C_0 increased from 379.6 for 0.1SLPM to 379.6, 113.3, 52.9, 30.2, and 26.7 for 0.5, 1, 2, and 5 SLPM, respectively. These results indicate that increasing the regeneration purge flow rate improves regeneration by increasing the concentration gradient between the adsorbent pores and the bulk purge gas. Desorbate concentration also decreases by increasing flow rate because of dilution effect (Lordgooei et al. 1996) which reduces the chance of coke formation. After some points, desorption concentration becomes relatively low and coke formation reaction rate decreases drastically. Increasing flow rate more than this point will not change regeneration performance anymore.

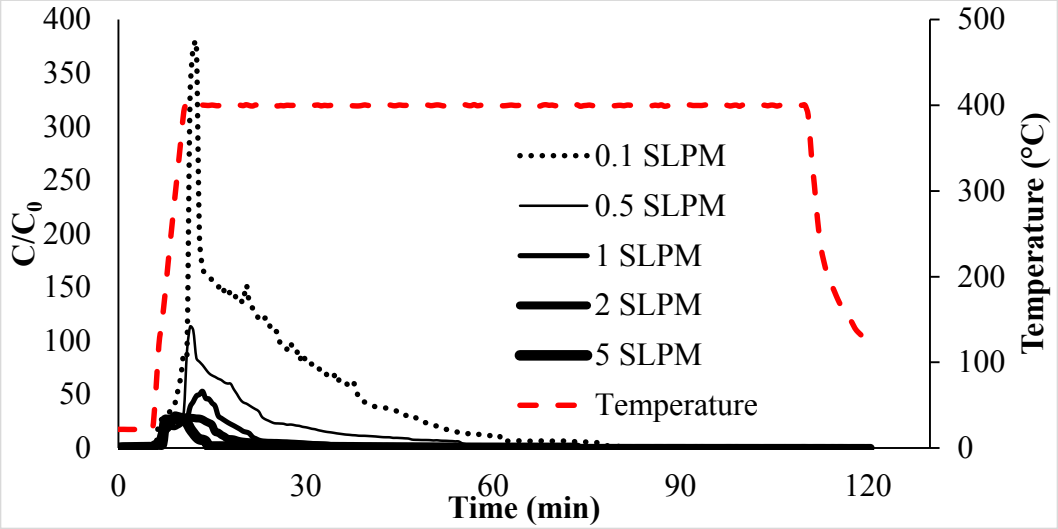

Figure 3-9. Concentration and temperature profile during regeneration of ACFC using different flow rates

Presented results clearly describe possible negatives associated with decreasing purge gas consumption or increasing heating rates during adsorbent regeneration. Fast regeneration methods such as microwave and resistive heating (Ania et al. 2004, Sullivan et al. 2004a, Sullivan et al. 2004b, Ania et al. 2005, Caliskan et al. 2012) can face some drawback in terms of loss of adsorption capacity, increased heel buildup, and shortened adsorbent lifetime if desorption concentration and mass transfer limitations are not considered. These results provide the first evidence that high desorbate concentration at high regeneration temperature can cause adsorbent deterioration during prolonged use, suggesting that flow and heating rates be carefully selected based on the specific adsorbent-adsorbate pair. Optimization of regeneration heating rate and purge gas flow rate make it possible to have fast heating with minimal adsorbent deterioration.

3-4. References

An, H. and B. Feng (2010). "Desorption of CO2 from activated carbon fibre–phenolic resin composite by electrothermal effect." International Journal of Greenhouse Gas Control **4**(1): 57-63.

Ania, C. O., J. A. Menendez, J. B. Parra and J. J. Pis (2004). "Microwave-induced regeneration of activated carbons polluted with phenol. A comparison with conventional thermal regeneration." Carbon **42**(7): 1383-1387.

Ania, C. O., J. B. Parra, J. A. Menendez and J. J. Pis (2005). "Effect of microwave and conventional regeneration on the microporous and mesoporous network and on the adsorptive capacity of activated carbons." Microporous and Mesoporous Materials **85**(1–2): 7-15.

Caliskan, E., J. M. Bermudez, J. B. Parra, J. A. Menendez, M. Mahramanlıoğlu and C. O. Ania (2012). "Low temperature regeneration of activated carbons using microwaves: Revising conventional wisdom." Journal of Environmental Management **102**(0): 134-140.

Carratala-Abril, J., M. A. Lillo-Rodenas, A. Linares-Solano and D. Cazorla-Amorós (2010). "Regeneration of activated carbons saturated with benzene or toluene using an oxygen-containing atmosphere." Chemical Engineering Science **65**(6): 2190-2198.

Dabrowski, A., P. Podkoscielny, Z. Hubicki and M. Barczak (2005). "Adsorption of phenolic compounds by activated carbon: a critical review." Chemosphere **58**(8): 1049-1070.

Dombrowski, K., C. Lehmann, P. Sullivan, D. Ramirez, M. Rood and K. Hay (2004). "Organic vapor recovery and energy efficiency during electric regeneration of an activated carbon fiber cloth adsorber." Journal of Environmental Engineering **130**(3): 268-275.

Fayaz, M., H. Wang, M. Lashaki, Z. Hashisho, J. H. Philips and J. E. Anderson (2011). Accumulation of Adsorbed of Organic Vapors from Automobile Painting Operations on Bead Activated Carbon. Air and Waste Management Association Annual Meeting Conference and Exhibition, Orlando.

Ferro-Garcia, M. A., J. P. Joly, J. Rivera-Utrilla and C. Moreno-Castilla (1995). "Thermal desorption of chlorophenols from activated carbons with different porosity." Langmuir **11**(7): 2648-2651.

Grant, T. M. and C. J. King (1990). "Mechanism of irreversible adsorption of phenolic compounds by activated carbons." Industrial & Engineering Chemistry Research **29**(2): 264-271.

Ha, S. R. and S. Vinitnantharat (2000). "Competitive removal of phenol and 2,4-dichlorophenol in biological activated carbon system." Environmental Technology **21**(4): 387-396.

Han, X., H. Lin and Y. Zheng (2014). "Understanding capacity loss of activated carbons in the adsorption and regeneration process for denitrogenation and desulfurization of diesel fuels." Separation and Purification Technology **133**(0): 194-203.

Hashisho, Z., M. J. Rood, S. Barot and J. Bernhard (2009). "Role of functional groups on the microwave attenuation and electric resistivity of activated carbon fiber cloth." Carbon **47**(7): 1814-1823.

Lashaki, M., M. Fayaz, H. Wang, Z. Hashisho, J. H. Philips, J. E. Anderson and M. Nichols (2012). "Effect of adsorption and regeneration temperature on irreversible adsorption of organic vapors on beaded activated carbon." Environmental Science & Technology **46**(7): 4083-4090.

Lordgooei, M., K. R. Carmichael, T. W. Kelly, M. J. Rood and S. M. Larson (1996). "Activated carbon cloth adsorption-cryogenic system to recover toxic volatile organic compounds." Gas Separation & Purification **10**(2): 123-130.

Lowell, S. and J. E. Shields (1991). Powder Surface Area and Porosity, Springer.

Lu, Q. and G. A. Sorial (2004a). "Adsorption of phenolics on activated carbon–impact of pore size and molecular oxygen." Chemosphere **55**(5): 671-679.

Lu, Q. and G. A. Sorial (2004b). "The role of adsorbent pore size distribution in multicomponent adsorption on activated carbon." Carbon **42**(15): 3133-3142.

Lu, Q. and G. A. Sorial (2007). "The effect of functional groups on oligomerization of phenolics on activated carbon." Journal of Hazardous Materials **148**(1–2): 436-445.

Mallouk, K. E., D. L. Johnsen and M. J. Rood (2010). "Capture and recovery of isobutane by electrothermal swing adsorption with post-desorption liquefaction." Environmental Science & Technology **44**(18): 7070-7075.

Ramos, M. E., P. R. Bonelli, A. L. Cukierman, M. M. L. Ribeiro Carrott and P. J. M. Carrott (2010). "Adsorption of volatile organic compounds onto activated carbon cloths derived from a novel regenerated cellulosic precursor." Journal of Hazardous Materials **177**(1–3): 175-182.

Roman, S., B. Ledesma, J. F. Gonzalez, A. Al-Kassir, G. Engo and A. Alvarez-Murillo (2013). "Two stage thermal regeneration of exhausted activated carbons. Steam gasification of effluents." Journal of Analytical and Applied Pyrolysis **103**(0): 201-206.

Sidheswaran, M. (2012). "Energy Efficient Indoor VOC Air Cleaning with Activated Carbon Fiber (ACF) Filters."

Subrenat, A., J. N. Baléo, P. Le Cloirec and P. E. Blanc (2001). "Electrical behaviour of activated carbon cloth heated by the joule effect: desorption application." Carbon **39**(5): 707-716.

Subrenat, A. and P. Le Cloirec (2004). "Adsorption onto activated carbon cloths and electrothermal regeneration: Its potential industrial applications." Journal of Environmental Engineering **130**(3): 249-257.

Sullivan, P., M. Rood, K. Dombrowski and K. Hay (2004a). "Capture of organic vapors using adsorption and electrothermal regeneration." Journal of Environmental Engineering **130**(3): 258-267.

Sullivan, P. D., M. J. Rood, G. Grevillot, J. D. Wander and K. J. Hay (2004b). "Activated carbon fiber cloth electrothermal swing adsorption system." Environmental Science & Technology **38**(18): 4865-4877.

Thakkar, S. and M. Manes (1987). "Adsorptive displacement analysis of many-component priority pollutants on activated carbon." Environmental Science Technology **21**(6): 546-549.

Vinitnantharat, S., A. Baral, Y. Ishibashi and S. R. Ha (2001). "Quantitative bioregeneration of granular activated carbon loaded with phenol and 2,4-dichlorophenol." Environmental Technology **22**(3): 339-344.

Yu, F. D., L. Luo and G. Grevillot (2007). "Electrothermal swing adsorption of toluene on an activated carbon monolith: Experiments and parametric theoretical study." Chemical Engineering and Processing: Process Intensification **46**(1): 70-81.

CHAPTER 4 CONCLUSIONS AND RECOMENDATIONS

4-1. Conclusions

The effect of regeneration conditions on heel buildup and adsorption capacity loss of activated carbon fiber cloth (ACFC) were investigated in this work. For this purpose, five adsorption/regeneration cycles were completed using 1,2,4-trimethylbenzene (TMB) as adsorbate. Regeneration experiments were completed using resistive heating at different desorption temperatures (288 °C and 400 °C), heating rates (5 to 100 °C/min), and flow rates (0.1 to 5 SLPM) to determine the effect of these parameters. Supporting experiments were also done using thermo-gravimetric analysis (TGA), scanning electron microscopy (SEM) and micropore surface analysis. Important findings of this research are:

- After regeneration at 288 °C, ACFC10's adsorption capacity loss was 82.6%, while the adsorption capacity loss for ACFC15 and ACFC20 (with larger pores) were 8.8% and 5.4%, respectively
- All three ACFC samples had similar cumulative heel (3-4 wt%) after five adsorption/regeneration cycling at 288 °C
- After regeneration at 400 °C, adsorption capacity losses for ACFC10, ACFC15, and ACFC20 were 93%, 51% and 50%, respectively and cumulative heel for ACFC10, ACFC15 and ACFC20 were 3.7 wt%, 10.4 wt% and 18.9 wt%, respectively.

- Reduction in breakthrough time of all three ACFCs also confirmed adsorption capacity loss data for both regeneration temperatures
- Comparing capacity loss and micropore surface analysis results indicates partial micropore obstruction of ACFC samples especially ACFC10 that prevent accessibility to bulky molecules but permit accessibility to smaller ones.
- TGA/DTG results confirmed that species formed during adsorption/regeneration cycling were strongly attached to the ACFC surface and cannot be removed even at temperatures as high as 900 °C
- Heel buildup and adsorption capacity loss increased from 4.6 to 10.4 wt% and from 7.8 to 52.0%, respectively, with increasing heating rate from 5 to 100 °C/min
- Increasing the purge gas flow rate (from 0.1 to 5 SLPM) has the opposite effect compared to heating rate, decreasing heel buildup (from 14.6 to 1.4%) and capacity loss (from 82.3 to 2.1%).
- Increasing heating rate increased maximum concentration during desorption as well as the temperature at which that maximum concentration occurred. Unlike the effect of heating rate, increasing flow rate decreased maximum concentration of desorbate during regeneration, resulting in smaller heel.

These results suggest that heel buildup and capacity loss of ACFC samples were the result of carbon deposition due to TMB degradation. Increasing regeneration temperature at high heating rate (70 °C/min) increased heel buildup and capacity loss because degradation of TMB is an endothermic reaction. Therefore, increasing temperature increased carbon deposition which obstructed the pores of ACFC samples. Carbon species formed during regeneration obstruct narrow micropores of ACFC10, however, the larger micropores of ACFC15 and ACFC20 can still accommodate additional adsorbate despite having similar amount of heel. The results of heating rate and flow rate indicated that exposure of more concentrated stream of TMB to higher temperatures during regeneration resulted in more thermal degradation of TMB. Therefore, increasing heating rate or/and decreasing flow rate increased heel buildup and capacity loss. These results could be used to optimize regeneration conditions for resistive heating to allow fast desorption with minimal desorbate decomposition and heel buildup.

4-2. Recommendations for Future Research

This research has highlighted several topics that need to investigate further in future works. The major research area are:

- Effect of surface functional group on organic vapor decomposition during regeneration of activated carbon adsorbent. The general understanding in the literature is that changing functional group on the surface of activated carbon can change the adsorbate-adsorbent interaction and the heel buildup. Therefore, the effect of this parameter should be investigated

- Presence of oxidizing gas such as carbon dioxide or presence of water at high temperature might oxidize the carbon species formed during regeneration. Hence, investigation of the effect of regeneration gas and humidity on organic vapor decomposition during regeneration of activated carbon adsorbent is recommended.
- Understanding the effect of adsorbate in organic compound degradation will help to find out a proper mechanism for this process. Therefore, Influence of adsorbate in coke formation during regeneration of activated carbon adsorbent should be investigated.

APPENDICES

Appendix A: five cycles of adsorption/desorption of 1,2,4-trimethylbenzene on ACFC at different regeneration temperatures

Table A- 1 Mass balance of 1,2,4- trimethylbenzene adsorption on ACFC10 and regeneration at 288 °C (1st run)

Weight of dry virgin ACFC: 5.4 g				
Cycle	Amount adsorbed (g)	% adsorption capacity (g adsorbed/ g adsorbent	Total Heel (g)	% accumulated heel formation (g adsorbate remained/ g adsorbent
1	1.02	18.89	0.06	1.11
2	0.97	17.96	0.14	2.59
3	0.49	9.07	0.18	3.33
4	0.20	3.70	0.18	3.33
5	0.10	1.85	0.18	3.33

Table A- 2 Mass balance of 1,2,4- trimethylbenzene adsorption on ACFC10 and regeneration at 288 °C (2nd run)

Weight of dry virgin ACFC: 6.4 g				
Cycle	Amount adsorbed (g)	% adsorption capacity (g adsorbed/ g adsorbent	Total Heel (g)	% accumulated heel formation (g adsorbate remained/ g adsorbent
1	1.28	19.94	0.08	1.25
2	1.03	16.04	0.16	2.49
3	0.51	7.94	0.16	2.49
4	0.29	4.52	0.24	3.74
5	0.09	1.40	0.24	3.74

Table A- 3 Mass balance of 1,2,4- trimethylbenzene adsorption on ACFC 15 and regeneration at 288 °C (1st run)

Weight of dry virgin ACFC: 5.7 g				
Cycle	Amount adsorbed (g)	% adsorption capacity (g adsorbed/ g adsorbent	Total Heel (g)	% accumulated heel formation (g adsorbate remained/ g adsorbent
1	1.79	31.51	0.11	1.94
2	1.70	29.93	0.17	2.99
3	1.67	29.40	0.19	3.35
4	1.63	28.70	0.20	3.52
5	1.64	28.87	0.25	4.40

Table A- 4 Mass balance of 1,2,4- trimethylbenzene adsorption on ACFC 15 and regeneration at 288 °C (2nd run)

Weight of dry virgin ACFC: 5.3 g				
Cycle	Amount adsorbed (g)	% adsorption capacity (g adsorbed/ g adsorbent	Total Heel (g)	% accumulated heel formation (g adsorbate remained/ g adsorbent
1	1.80	34.09	0.11	2.08
2	1.75	33.14	0.18	3.41
3	1.70	32.20	0.24	4.55
4	1.67	31.63	0.24	4.55
5	1.67	31.63	0.24	4.55

Table A- 5 Mass balance of 1,2,4- trimethylbenzene adsorption on ACFC 20 and regeneration at 288 °C (1st run)

Weight of dry virgin ACFC: 3.2 g				
Cycle	Amount adsorbed (g)	% adsorption capacity (g adsorbed/ g adsorbent	Total Heel (g)	% accumulated heel formation (g adsorbate remained/ g adsorbent
1	1.56	47.85	0.05	1.53
2	1.53	46.93	0.09	2.76
3	1.49	45.71	0.13	3.99
4	1.48	45.40	0.14	4.29
5	1.50	46.01	0.15	4.60

Table A- 6 Mass balance of 1,2,4- trimethylbenzene adsorption on ACFC 20 and regeneration at 288 °C (2nd run)

Weight of dry virgin ACFC: 3.3 g				
Cycle	Amount adsorbed (g)	% adsorption capacity (g adsorbed/ g adsorbent	Total Heel (g)	% accumulated heel formation (g adsorbate remained/ g adsorbent
1	1.67	50.64	0.06	1.82
2	1.62	49.12	0.11	3.34
3	1.59	48.21	0.12	3.64
4	1.57	47.60	0.13	3.94
5	1.57	47.60	0.15	4.34

Table A- 7 Mass balance of 1,2,4- trimethylbenzene adsorption on ACFC10 and regeneration at 400 °C (1st run)

Weight of dry virgin ACFC: 5.4 g				
Cycle	Amount adsorbed (g)	% adsorption capacity (g adsorbed/ g adsorbent	Total Heel (g)	% accumulated heel formation (g adsorbate remained/ g adsorbent
1	1.07	19.71	0.12	2.21
2	0.44	8.10	0.13	2.39
3	0.22	4.05	0.14	2.58
4	0.10	1.84	0.16	2.95
5	0.07	1.29	0.18	3.31

Table A- 8 Mass balance of 1,2,4- trimethylbenzene adsorption on ACFC10 and regeneration at 400 °C (2nd run)

Weight of dry virgin ACFC: 5.4 g				
Cycle	Amount adsorbed (g)	% adsorption capacity (g adsorbed/ g adsorbent	Total Heel (g)	% accumulated heel formation (g adsorbate remained/ g adsorbent
1	1.13	20.81	0.14	2.58
2	0.81	14.92	0.18	3.31
3	0.35	6.45	0.20	3.68
4	0.23	4.24	0.20	3.68
5	0.19	3.50	0.23	4.24

Table A- 9 Mass balance of 1,2,4- trimethylbenzene adsorption on ACFC15 and regeneration at 400 °C

Weight of dry virgin ACFC: 4.4 g				
Cycle	Amount adsorbed (g)	% adsorption capacity (g adsorbed/ g adsorbent	Total Heel (g)	% accumulated heel formation (g adsorbate remained/ g adsorbent
1	1.47	33.18	0.19	4.29
2	1.36	30.70	0.28	6.32
3	1.10	24.83	0.33	7.45
4	0.95	21.44	0.42	9.48
5	0.72	16.25	0.46	10.38

Table A- 10 Mass balance of 1,2,4- trimethylbenzene adsorption on ACFC20 and regeneration at 400 °C

Weight of dry virgin ACFC: 3.3 g				
Cycle	Amount adsorbed (g)	% adsorption capacity (g adsorbed/ g adsorbent	Total Heel (g)	% accumulated heel formation (g adsorbate remained/ g adsorbent
1	1.69	51.52	0.15	4.57
2	1.61	49.09	0.30	9.15
3	1.50	45.73	0.46	14.02
4	1.17	35.67	0.60	18.29
5	0.84	25.61	0.62	18.90

Appendix B: five cycles of adsorption/desorption of 1,2,4-trimethylbenzene on ACFC15 at different heating rates

Table B- 1 Mass balance of 1,2,4- trimethylbenzene adsorption on ACFC15 at 400 °C for heating rate of 5 °C/min

Weight of dry virgin ACFC: 4.1 g				
Cycle	Amount adsorbed (g)	% adsorption capacity (g adsorbed/ g adsorbent	Total Heel (g)	% accumulated heel formation (g adsorbate remained/ g adsorbent
1	1.38	33.74	0.03	0.73
2	1.37	33.50	0.07	1.71
3	1.33	32.52	0.13	3.18
4	1.27	31.05	0.14	3.42
5	1.27	31.05	0.19	4.65

Table B- 2 Mass balance of 1,2,4- trimethylbenzene adsorption on ACFC15 at 400 °C for heating rate of 10 °C/min

Weight of dry virgin ACFC: 4.4 g				
Cycle	Amount adsorbed (g)	% adsorption capacity (g adsorbed/ g adsorbent	Total Heel (g)	% accumulated heel formation (g adsorbate remained/ g adsorbent
1	1.37	31.21	0.09	2.05
2	1.30	29.61	0.14	3.19
3	1.25	28.47	0.18	4.10
4	1.20	27.33	0.25	5.69
5	1.11	25.28	0.30	6.83

Table B- 3 Mass balance of 1,2,4- trimethylbenzene adsorption on ACFC15 at 400 °C for heating rate of 20 °C/min

Weight of dry virgin ACFC: 4.7 g				
Cycle	Amount adsorbed (g)	% adsorption capacity (g adsorbed/ g adsorbent	Total Heel (g)	% accumulated heel formation (g adsorbate remained/ g adsorbent
1	1.45	30.85	0.08	1.70
2	1.40	29.79	0.22	4.68
3	1.29	27.45	0.30	6.38
4	0.92	19.57	0.37	7.87
5	0.68	14.47	0.41	8.72

Table B- 4 Mass balance of 1,2,4- trimethylbenzene adsorption on ACFC15 at 400 °C for heating rate of 40 °C/min

Weight of dry virgin ACFC: 4.9 g				
Cycle	Amount adsorbed (g)	% adsorption capacity (g adsorbed/ g adsorbent	Total Heel (g)	% accumulated heel formation (g adsorbate remained/ g adsorbent
1	1.60	32.45	0.10	2.03
2	1.50	30.43	0.22	4.46
3	1.27	25.76	0.33	6.69
4	0.92	18.66	0.38	7.71
5	0.77	15.62	0.48	9.74

Table B- 5 Mass balance of 1,2,4- trimethylbenzene adsorption on ACFC15 at 400 °C for heating rate of 70 °C/min

Weight of dry virgin ACFC: 4.4 g				
Cycle	Amount adsorbed (g)	% adsorption capacity (g adsorbed/ g adsorbent	Total Heel (g)	% accumulated heel formation (g adsorbate remained/ g adsorbent
1	1.47	33.18	0.19	4.29
2	1.36	30.70	0.28	6.32
3	1.10	24.83	0.33	7.45
4	0.95	21.44	0.42	9.48
5	0.72	16.25	0.46	10.38

Table B- 6 Mass balance of 1,2,4- trimethylbenzene adsorption on ACFC15 at 400 °C for heating rate of 100 °C/min

Weight of dry virgin ACFC: 4.8 g				
Cycle	Amount adsorbed (g)	% adsorption capacity (g adsorbed/ g adsorbent	Total Heel (g)	% accumulated heel formation (g adsorbate remained/ g adsorbent
1	1.61	33.47	0.13	2.70
2	1.50	31.19	0.30	6.24
3	1.37	28.48	0.39	8.11
4	1.10	22.87	0.48	9.98
5	0.78	16.22	0.51	10.60

Appendix C: five cycles of adsorption/desorption of 1,2,4-trimethylbenzene on ACFC15 at different flow rates

Table C- 1 Mass balance of 1,2,4- trimethylbenzene adsorption on ACFC15 at 400 °C for flow rate of 0.1 SLPM

Weight of dry virgin ACFC: 4.9 g				
Cycle	Amount adsorbed (g)	% adsorption capacity (g adsorbed/ g adsorbent	Total Heel (g)	% accumulated heel formation (g adsorbate remained/ g adsorbent
1	1.64	33.74	0.52	10.70
2	0.78	16.05	0.62	12.76
3	0.58	11.93	0.64	13.17
4	0.51	10.49	0.66	13.58
5	0.29	5.97	0.71	14.61

Table C- 2 Mass balance of 1,2,4- trimethylbenzene adsorption on ACFC15 at 400 °C for flow rate of 0.5 SLPM

Weight of dry virgin ACFC: 4.5 g				
Cycle	Amount adsorbed (g)	% adsorption capacity (g adsorbed/ g adsorbent	Total Heel (g)	% accumulated heel formation (g adsorbate remained/ g adsorbent
1	1.55	34.37	0.18	3.99
2	1.42	31.49	0.37	8.20
3	0.74	16.41	0.47	10.42
4	0.55	12.20	0.49	10.86
5	0.56	12.42	0.52	11.53

Table C- 3 Mass balance of 1,2,4- trimethylbenzene adsorption on ACFC15 at 400 °C for flow rate of 1 SLPM

Weight of dry virgin ACFC: 4.4 g				
Cycle	Amount adsorbed (g)	% adsorption capacity (g adsorbed/ g adsorbent	Total Heel (g)	% accumulated heel formation (g adsorbate remained/ g adsorbent
1	1.47	33.18	0.19	4.29
2	1.36	30.70	0.28	6.32
3	1.10	24.83	0.33	7.45
4	0.95	21.44	0.42	9.48
5	0.72	16.25	0.46	10.38

Table C- 4 Mass balance of 1,2,4- trimethylbenzene adsorption on ACFC15 at 400 °C for flow rate of 2 SLPM

Weight of dry virgin ACFC: 4.5 g				
Cycle	Amount adsorbed (g)	% adsorption capacity (g adsorbed/ g adsorbent	Total Heel (g)	% accumulated heel formation (g adsorbate remained/ g adsorbent
1	1.35	30.78	0.02	0.44
2	1.32	29.33	0.06	1.33
3	1.30	28.89	0.09	2.00
4	1.30	28.89	0.11	2.44
5	1.28	28.44	0.13	2.89

Table C- 5 Mass balance of 1,2,4- trimethylbenzene adsorption on ACFC15 at 400 °C for flow rate of 5 SLPM

Weight of dry virgin ACFC: 4.4 g				
Cycle	Amount adsorbed (g)	% adsorption capacity (g adsorbed/ g adsorbent	Total Heel (g)	% accumulated heel formation (g adsorbate remained/ g adsorbent
1	1.47	33.33	0.01	0.23
2	1.47	33.33	0.02	0.45
3	1.45	32.88	0.04	0.91
4	1.44	32.65	0.05	1.13
5	1.44	32.65	0.06	1.36